Schouten Henk J. (Orcid ID: 0000-0003-4495-1951)
Usadel Björn (Orcid ID: 0000-0003-0921-8041)
Underwood Charles J. (Orcid ID: 0000-0001-5730-6279)

A chromosome scale tomato genome built from complementary PacBio and Nanopore sequences alone reveals extensive linkage drag during breeding

Willem M. J. van Rengs[1,‡], Maximilian H.-W. Schmidt[2,‡], Sieglinde Effgen[1], Duyen Bao Le[5], Yazhong Wang[1], Mohd Waznul Adly Mohd Zaidan[1], Bruno Huettel[3], Henk J. Schouten[4], Björn Usadel[2,5]* and Charles J. Underwood[1]*

[1]Department of Chromosome Biology, Max Planck Institute for Plant Breeding Research, Carl-von-Linné-Weg 10, 50829, Cologne, Germany

[2]IBG-4 Bioinformatics, Forschungszentrum Jülich, 52428 Jülich, Germany

[3]Max Planck-Genome-center Cologne, Carl-von-Linné-Weg 10, 50829 Cologne, Germany

[4]Department of Plant Breeding, Wageningen University and Research, P.O. Box 386, 6700 AJ, Wageningen, The Netherlands

[5]Heinrich Heine University Düsseldorf, Institute of Biological Data Science, Düsseldorf, Germany

‡ These authors contributed equally

Running title: Long-read-only tomato genome reveals linkage drag

Keywords (10): *Solanum lycopersicum*, *Solanum peruvianum,* PacBio, SMRT sequencing, Oxford Nanopore Technologies, Nanopore sequencing, Genome assembly, Linkage drag, Plant breeding, Tobacco mosaic virus.

***Corresponding authors**:
Björn Usadel (b.usadel@fz-juelich.de) and Charles J. Underwood (cunderwood@mpipz.mpg.de)

Abstract

The assembly and scaffolding of plant crop genomes facilitate the characterization of genetically diverse cultivated and wild germplasm. The cultivated tomato has been improved through the introgression of genetic material from related wild species, including resistance to pandemic strains of Tobacco Mosaic virus (TMV) from *Solanum peruvianum*. Here we applied PacBio HiFi and ONT nanopore sequencing to develop independent, highly contiguous and complementary assemblies of an inbred TMV-resistant tomato variety. We show specific examples of how HiFi and ONT datasets can complement one another to improve assembly contiguity. We merged the HiFi and ONT assemblies to generate a long-read-only assembly where all twelve chromosomes were represented as twelve contiguous sequences (N50=68.5 Mbp). This chromosome scale assembly did not require scaffolding using an orthogonal data type. The merged assembly was validated by chromosome conformation capture data and is highly consistent with previous tomato genome assemblies that made use of genetic maps and

HiC for scaffolding. Our long-read-only assembly reveals that a complex series of structural variants linked to the TMV resistance gene likely contributed to linkage drag of a 64.1 Mbp region of the *S. peruvianum* genome during tomato breeding. Through marker studies and ONT-based comprehensive haplotyping we show that this minimal introgression region is present in six cultivated tomato hybrid varieties developed in three commercial breeding programs. Our results suggest that complementary long read technologies can facilitate the rapid generation of near complete genome sequences.

Introduction

DNA sequencing technology has evolved rapidly in the last two decades, and long read DNA sequencing has fundamentally altered approaches in genome assembly. Long DNA sequence reads that can span repeated sequences, including the full length of transposable elements, can simplify the assembly process (Koren *et al.*, 2012; Dumschott *et al.*, 2020). Pacific Biosciences (PacBio) initially delivered long yet error prone reads (initially with a raw base accuracy of 82.1 – 84.6%) facilitating short-long read hybrid assembly and long-read-only assembly approaches (Koren *et al.*, 2012; Berlin *et al.*, 2015). Whilst this was also rapidly adopted in the field of plant genomics (Zapata *et al.*, 2016; Vanburen *et al.*, 2015), the application of nanopore sequencing developed by Oxford Nanopore Technologies (ONT) led to long read sequencing with minimal capital outlay (Schmidt *et al.*, 2017; Michael *et al.*, 2018). Increases in sequencing yield and improvements in raw base accuracy, as well as protocol development for DNA extraction (Vaillancourt and Buell, 2019; Vilanova *et al.*, 2020), have facilitated the analysis of crop pangenomes (Alonge *et al.*, 2020; Qin *et al.*, 2021; Liu *et al.*, 2020), and the development of near-complete human and Arabidopsis genome sequences (Nurk *et al.*, 2021; Naish *et al.*, 2021).

The PacBio Sequel II platform now delivers long High Fidelity (HiFi) reads with a low error rate. HiFi reads are a consensus of multiple passes of the same circular DNA molecule, typically with a 10-20 kbp genomic DNA insert, and therefore have a much higher per base accuracy (99.5 - 99.9%) than the individual passes (85%) (Vollger *et al.*, 2020; Hon *et al.*, 2020). The length and low error rate of HiFi reads means that they span the majority of repeated sequences and can also differentiate between highly similar repeated sequences. Various assembly tools have been developed to harness the characteristics of HiFi reads (Cheng *et al.*, 2021; Nurk *et al.*, 2020). HiFi reads are restricted in length because larger DNA insert sizes are sequenced with a lower number of passes, due to limitations of DNA polymerase processivity. ONT has recently relaunched a form of two pass consensus sequencing but has largely focused on applying deep learning to improve raw read base accuracy to 97% and new Q20+ chemistry is beginning to deliver the promised 99% accuracy. ONT sequencing does not yet provide a raw base accuracy high enough to use the same assembly tools that are used for HiFi reads, yet can generate reads that are multiple megabases in length that can reliably align to reference genomes (Payne *et al.*, 2019). ONT reads in the 20 kbp - 200 kbp category can span complex tandem arrays of repeated sequences that litter plant genomes. Therefore, current long read sequencing options are either very high-quality reads between the length of 10-20 kbp (HiFi) or considerably longer reads with lower per base accuracy (ONT). Despite the apparently complementary strengths of HiFi and ONT data, there have been few attempts to combine the two data types in genome assemblies.

Tomato (*Solanum lycopersicum*) fruits are an important source of vitamins and minerals in a balanced diet and are, globally, the most produced crop in the vegetable category (Costa and Heuvelink, 2018). Tomato varieties can be improved by the introgression of novel resistances to abiotic and biotic stresses from multiple related wild species (Bai and Lindhout, 2007; Peralta *et al.*, 2008; Li *et al.*, 2010; Foolad *et al.*, 1997). High quality reference genomes are available for the cultivated tomato, *S. lycopersicum* cv. ‘Heinz 1706’ (SL4.0) (Sato *et al.*, 2012; Hosmani *et al.*, 2019), the closely related red-fruited *S. pimpinellifolium* ‘LA2093’ (X., Wang *et al.*, 2020), the more distantly related green fruited *S. pennellii* ‘LA0716’ (Bolger *et al.*, 2014) and the purple/black fruited *S. lycopersicoides* ‘LA2951’ (Powell *et al.*, 2020). Alongside these reference genomes, more than 1000 tomato varieties and wild tomato species have been sequenced on Illumina platforms (Gao *et al.*, 2019; Aflitos *et al.*, 2014; Lin *et al.*, 2014) and a panel of 100 of these were recently sequenced using ONT long reads to characterize structural variants (Alonge *et al.*, 2020). In summary, cultivated and wild tomato genomes have been extensively characterized to understand genetic diversity yet even the SL4.0 reference genome contains gaps in repetitive regions, including subtelomeric and centromeric regions.

Tobamoviruses are single stranded RNA viruses that can be devastating pathogens for tomato and other vegetable crops. The tobacco mosaic virus (TMV) and tomato mosaic virus (ToMV) are two tobamoviruses that can infect susceptible tomato cultivars and lead to substantial yield reduction (Lanfermeijer *et al.*, 2005; Lanfermeijer *et al.*, 2003). From the 1930s until the 1960s tomato breeders searched for TMV resistance in various wild tomato species, including *S. pimpinellifolium, S. pennellii, S. habrochaites* (syn. *L. hirsutum*), *S. chilense* and *S. peruvianum* (Pelham, 1966). TMV resistance was found including in *S. pennellii*, *S. habrochaites* (*Tm-1*) and *S. peruvianum* (allelic resistance genes *Tm-2* and *Tm-2*^{2}) (Pelham, 1966; Lanfermeijer *et al.*, 2005). Of the three known TMV resistance genes, introgression of *Tm-2*^{2} from *S. peruvianum* (accession P. I. 128650) has provided dominant, robust and lasting resistance to all TMV and ToMV strains since its discovery in the 1960s and therefore most modern tomato greenhouse varieties contain the *Tm-2*^{2} gene (Alexander, 1963; Schouten *et al.*, 2019). The *Tm-2*^{2} gene encodes a coiled-coil domain Nod-like receptor (CC-NLR) protein that recognizes the movement protein (MP), a key viral protein that facilitates TMV/ToMV movement between plant cells via plasmodesmata (J., Wang *et al.*, 2020; Lanfermeijer *et al.*, 2003; Lanfermeijer *et al.*, 2005). The exact size and the structure of the introgression containing the *Tm-2*^{2} gene has remained unknown, although it was known to include at least half of the physical length of chromosome 9 (Schouten *et al.*, 2019; Lin *et al.*, 2014).

Here we sequenced and assembled the genome of the *S. lycopersicum* cultivar Moneyberg-TMV (see Materials and methods for breeding history), a popular line used in tomato research because of its vigour, homozygosity and capacity for genetic transformation. PacBio HiFi and ONT nanopore sequencing reads were independently used to develop highly contiguous genome assemblies. We merged HiFi and ONT assemblies to develop a long-read-only assembly (‘MbTMV’) where all twelve chromosomes were present as single contigs without the introduction of artificial gaps. The MbTMV assembly was validated through orthogonal approaches including chromosome conformation capture data, mapping of raw long read data and coverage analysis, and extensive comparison with the SL4.0 assembly. Through our long-read-only assembly and the analysis of six commercial tomato hybrids, we show that a minimal 64.1 Mbp introgression has been dragged along with the *Tm-2*^{2} gene despite more than fifty years of tomato breeding.

Results

“Long-read-only” genome assembly, validation and analysis

We generated long read DNA sequences of the *S. lycopersicum* cv. ‘Moneyberg-TMV’ genome using two different third generation sequencing technologies. High molecular weight (HMW) DNA was extracted and used to construct HiFi sequencing libraries where we made use of two different insert sizes to balance read length and read quality. The two libraries were subjected to PacBio HiFi sequencing on two Sequel II SMRT cells. The first cell yielded 18.8 Gbp with a HiFi read length N50 of 13.9 kbp and mean quality (Q-value) of 28.59 (Table 1). The second cell yielded 21.8 Gbp of data with a HiFi read length N50 of 24.8 kbp and mean Q-value of 24.65 (Table 1). Using the same HMW DNA two identical nanopore library preparations were performed and subjected to ONT long read sequencing on two PromethION cells. This yielded 100.5 and 101.1 Gbp with respective read length N50 of 41.6 and 42.4 kbp, and mean Q-values of 11.28 and 11.18 (Table 1).

We used two genome assembly tools to assemble the HiFi reads and two different tools to assemble the ONT data, and compared the respective outcomes. PacBio HiFi reads were independently assembled using Hifiasm (Cheng *et al.*, 2021) and Canu (Nurk *et al.*, 2020), with respective N50 values of 31.3 and 17 Mbp (Table 2). Both HiFi assemblies contained single contigs that spanned the full length of the SL4.0 reference chromosome 5 (Supplementary Fig. 1). We checked for the completeness of the assembly of gene sequences by Benchmarking Universal Single Copy Orthologs (BUSCO) analysis (Simão *et al.*, 2015) which showed both assemblies were almost gene complete (both 98.4%), slightly improving upon the SL4.0 genome and comparable to the *S. pimpinellifolium* ‘LA2093’ genome (Table 2 & 3). Due to the lower base accuracy of the ONT reads different assembly tools were used in the assembly process. ONT reads were independently assembled using Flye (Kolmogorov *et al.*, 2019) and NECAT (Chen *et al.*, 2021), with respective N50 values of 18.9 and 50.2 Mbp (Table 2). The NECAT assembly contained single contigs that spanned the length of SL4.0 chromosomes 5 and 7 (Supplementary Fig. 1). While the NECAT ONT assembly was more contiguous than either of the HiFi assemblies, gene completeness was lower in both the raw Flye (97.8%) and NECAT (97.1%) assemblies (Table 2), but polishing was able to improve these values. All four assemblies were aligned against the SL4.0 genome and were found to be collinear, irrespective of technology or assembly tool used, except for chromosome 9 where the *S. peruvianum* introgression resides, indicative of mostly correct assemblies (Supplementary Fig. 1).

To test whether sequencing coverage was saturating, we randomly downsampled the HiFi and ONT data sets in intervals of 10% (from 90% down to 10%). Subsequently, we performed 9 Hifiasm and 9 NECAT assemblies on the respective downsampled datasets (Supplementary Table 1 & 2). For Hifiasm, we found that downsampling to as little as 50% (20.3 Gbp; about 24x coverage) of the full HiFi dataset only had a marginal effect on contiguity, indicating that the coverage was saturating (Supplementary Table 1). For NECAT, which internally selects the longest 40x coverage for assembly, we noticed that downsampling to even just 30% (49.7 Gbp; about 60x coverage) again only had a marginal effect on contiguity. However, care must be taken to avoid NECAT assembly artifacts that occasionally happen even at high coverage (Supplementary Table 2).

The dotplots of the HiFi and ONT assemblies revealed partial complementarity of the assemblies as the breakpoints were different (Supplementary Fig. 1 and Supplementary Dataset 1). To test for complementarity in the assemblies, we designed and implemented an assembly and polishing pipeline that merged the initial assemblies from the two different sequencing platforms (Fig. 1a, Supplementary Fig. 2, Supplementary Dataset 2 & Materials and Methods). In the final merged assembly, henceforth referred to as “MbTMV”, 98.9% of the assembly was represented in 12 contigs (N50=68.5 Mbp), all with a length of at least 52.2 Mbp, strongly suggestive of a near complete contig assembly (Table 3). The MbTMV assembly integrated sequences from all four (Hifiasm, Canu, Flye and NECAT) assembly tools (Supplementary Table 3). Strikingly, when the MbTMV assembly was aligned against the SL4.0 genome assembly the twelve tomato chromosomes were represented as twelve contigs (Fig. 1b), as expected from chromosome counting (Fig. 1c). 54 contigs making up 8.56 Mbp of sequence were not placed in the twelve major contigs and largely represented chloroplast, mitochondrial, rDNA and satellite repeat derived sequences (Supplementary Table 4). The unplaced contigs contained just a single complete unique BUSCO gene (of 5950 searched) implicating that the twelve contig assembly is near complete.

In order to test the structure of the obtained MbTMV assembly we made use of orthogonal approaches. We generated high resolution Omni-C (chromosome conformation capture) data (27.3x coverage) and aligned the paired reads to the MbTMV assembly, and assessed the resulting contact map (see Materials and Methods). The contact map provided strong support of twelve well assembled chromosomes, with no changes suggested (Fig. 2a). In addition, as validation alone, reference-based (SL4.0) scaffolding of the merged MbTMV assembly was performed, and did not break or improve the assembly (Supplementary Table 5).

We further checked the assembly by mapping the raw HiFi and ONT reads back to the MbTMV assembly to assess read coverage across the assembly. Indicative of an almost complete assembly, we found mostly even coverage across all twelve chromosomes (Fig. 2b & Supplementary Fig. 3), except in a few regions that are notoriously difficult to assemble. Higher ONT coverage was found on chromosome 1 and 2 overlapping with the highly repetitive 5S rDNA and 45S rDNA regions, respectively (Fig. 2b, Supplementary Fig. 3 and Supplementary Fig. 4) (Zhong *et al.*, 1998; Schmidt-Puchta *et al.*, 1989; Perry and Palukaitis, 1990; Chang *et al.*, 2008). A peak of HiFi and ONT coverage on chromosome 11 corresponded to a partial insertion of the mitochondrial genome, that has also been reported in the SL2.50 and SL4.0 assemblies (Fig. 2b & Supplementary Fig. 3) (Hosmani *et al.*, 2019; Kim and Lee, 2018). Lower than average HiFi and ONT coverage was found adjacent to centromeric TGR4-dense regions on chromosomes 6, 8 and 11, likely due to difficulties in assembling tandem arrays of 45S rDNA derived satellite repeats that are known to occur in three clusters in the tomato genome (Fig. 2b) (Jo *et al.*, 2009). However, other complete chromosomes (including 3, 5, 7, 9 and 10) had very stable coverage even over centromeric regions, indicating near complete assemblies (Fig. 2b & Supplementary Fig. 3). Further to this, we were able to find clusters of TGR1 in all subtelomeric regions apart from one end of chromosome 1 and both ends of chromosome 2, reflecting published FISH results (Fig. 2b)(Zhong *et al.*, 1998). We also found long tandem arrays of the telomeric repeat ($(TTTAGGG)_n$), on 14 of the 24 chromosome ends (Fig. 2b) (Ganal *et al.*, 1991).

Next, we assessed how the different sequencing technologies and assembly tools complement one another and make scaffolding obsolete. The merged assembly had sequence contributed from all four assembly tools (Supplementary Table 3), yet the polishing of ONT assemblies by all ONT and HiFi data (see Materials and Methods) ensured no drop in BUSCO completeness in the final merged sequence compared to raw HiFi assemblies (Table 2 & 3). In multiple cases where Hifiasm and Canu HiFi assemblies broke, ONT assemblies contained a multi-kilobase AT-rich sequence that was covered by even ONT read coverage, while HiFi read coverage steeply dropped in these regions (Supplementary Fig. 5a-c). An additional multi-kilobase CT/GA simple sequence repeat assembled from ONT reads (and with even ONT read coverage) was not assembled by Hifiasm and Canu, again due to a steep drop in HiFi read coverage (Supplementary Fig. 5d). Opposite to the previous examples, a NECAT assembly breakpoint was assembled from, and evenly covered by, HiFi reads (Supplementary Fig. 5e), further demonstrating the two sequencing technologies can be complementary.

Next, we performed in-depth analysis of the MbTMV genome structure and repeat content. We aligned MbTMV with SL4.0 and identified syntenic regions, SNPs, insertions, deletions and other structural variations such as duplications, translocations and inversions (Fig. 2d & Supplementary Dataset 3). Highly increased variation is observed on chromosome 9, where the *S. peruvianum* introgression is located, with a series of large inversions and extended non-syntenic regions (Fig. 2d & Supplementary Dataset 3). All other chromosomes were highly syntenic between the MbTMV assembly and SL4.0, except for a number of duplications that were identified (Fig. 2d). Strikingly, Hifiasm (HiFi), Canu (HiFi) and NECAT (ONT) all led to near-identical assemblies of tandemly repeated sequences in the TGR4-dense centromere of chromosome 5, which was also represented in the final MbTMV merged assembly, adding confidence that the centromere had been spanned in full (Fig. 2e, Fig. 2f & Supplementary Fig. 6). Finally, chromosome lengths were compared with three “gold standard” tomato species genomes (Fig. 2c). MbTMV had slightly longer chromosomes than the SL4.0 and *S. pimpinellifolium* ‘LA2093’ genomes in all cases except for chromosome 2. We suspected this could be related to a better assembly of repeat content, including the subtelomeres and telomeres, but also Long Terminal Repeat (LTR) transposable elements. Consistent with this, we found that the MbTMV assembly had the highest LTR Assembly Index (LAI) value (Table 3) (Ou *et al.*, 2018). The MbTMV chromosome 9, containing the introgression, was roughly 15.25 Mb longer than that from SL4.0 and similar in size to that from *S. pennellii* ‘LA0716’ (Fig. 2c). In summary, the MbTMV genome sequence represents a near complete assembly of all tomato genes and nuclear chromosomes.

In depth analysis of an alien introgression from *S. peruvianum*

The *Tm-2*^{2} gene confers broad resistance to TMV and ToMV and is located within a large introgression from *S. peruvianum* on chromosome 9, yet the full sequence and structure of the region is not known (Lin *et al.*, 2014). We re-aligned chromosome 9 sequences from MbTMV and SL4.0, called variants and used polymorphism density to map the exact break points of the introgression. This revealed that the introgression from

S. peruvianum is 64.1 Mbp (Fig. 3a, Supplementary Fig. 7 & Supplementary Dataset 4). The *S. peruvianum* sequence contains several large inversions compared to SL4.0, but the *Tm-2*^{2} gene is located within a syntenic region (Fig. 3a). To better understand the local context of the *Tm-2*^{2} gene in the fully assembled chromosome, we performed further alignments between MbTMV and SL4.0 sequences from ~10 Mbp and ~1 Mbp regions centered upon the *Tm-2*^{2} gene (Fig. 3b, 3c). Immediately at the start of the introgression, a drop in synteny is observed due to a series of insertions in the *S. peruvianum* derived sequence, followed by several large insertions and deletions, and two large inversions (Fig. 3b & Supplementary Dataset 5). At the local scale, the *Tm-2*^{2} gene is located within a syntenic region of about 150.5 kbp that is immediately adjacent to a non-syntenic region that is estimated to be 101.7 kbp longer in *S. peruvianum* (Fig. 3c & Supplementary Dataset 6). We validated our chromosome 9 assembly by aligning ONT reads from a different inbred variety (LYC 1969) that contains the *Tm-2*^{2} gene and a variety that does not (M82), and only found even coverage along chromosome 9 with the LYC 1969 sample, as expected (Supplementary Fig. 8)(Alonge *et al.*, 2020). Further to this, we aligned unassembled short DNA sequences from two other greenhouse tomato cultivars harboring the *Tm-2*^{2} gene, Moneymaker-TMV (MmTMV) and Merlice, with SL4.0. We found that the MmTMV introgression appears to be identical to that found in our MbTMV assembly, whereas the Merlice introgression is estimated to be at least 2.67 Mbp longer (Fig. 3d & Supplementary Fig. 7).

Genotyping and haplotyping the alien introgression in modern tomato hybrids

The *Tm-2*^{2} gene is present in the majority of modern tomato greenhouse cultivars, therefore we set out to check the size of the introgression in five commercial hybrids that were generated in three different breeding programs (Fig. 4a, 4b, Supplementary Fig. 9). To this end we used our assembly to design two polymorphic markers: one at the upstream extreme of the introgression (M-1) and a second at the downstream extreme of the introgression (M-2) (Fig. 3a). Using a published marker within the *Tm-2*^{2} gene (M-TM2^2, Fig. 3a), we found that all five hybrids contained the *Tm-2*^{2} gene, two in the heterozygous state (both produced by Syngenta), whereas the other three were homozygous (Fig. 4a, 4b & Supplementary Fig. 9). The two hybrids heterozygous for the M-TM2^2 marker were also heterozygous at M-1 and M-2, while the other three hybrids were homozygous at M-1 and M-2 (Fig. 4b & Supplementary Fig. 9). The absolute genetic linkage of the three markers in three different, and heavily resourced, tomato breeding programs confirms that conventional backcross breeding has been unable to break down the introgression.

In order to validate the marker genotyping at the chromosome scale, we haplotyped the alien introgression in one of the hemizygous commercial hybrids (*S. lycopersicum* cv. 'Funtelle') using ONT long reads. HMW DNA from the Funtelle hybrid was extracted, then ONT long reads were generated and assembled using Flye (Fig. 4c). The raw assembled contigs were aligned to the MbTMV and SL4.0 sequences and used to extract all contigs aligning to the respective chromosome 9 sequences (Fig. 4c). When these contig sequences were competitively re-aligned to the MbTMV and SL4.0 chromosome 9 sequences (Fig. 4c) we found both haplotypes were almost completely covered (Fig. 4d). Together, the marker studies (Fig. 4b & Supplementary Fig. 9) and analysis of the assembled ONT sequences (Fig. 4d) demonstrate that the full introgression is present in a heterozygous state, and that ONT reads can discriminate between related haplotypes in hybrid plants.

Discussion

Here, we have assembled a tomato genome *de novo* to chromosome level contigs using long read DNA sequences alone. The raw HiFi and ONT assemblies were highly contiguous and had different breakpoints in the respective assemblies, therefore merging the assemblies led to further increases in contiguity. Our merged assembly compares favourably (using BUSCO, LAI and chromosome length metrics) with previous tomato genome assemblies that relied on reference- or HiC-based scaffolding (Hosmani *et al.*, 2019; X., Wang *et al.*, 2020; Bolger *et al.*, 2014; Schmidt *et al.*, 2017; Alonge *et al.*, 2020; Alonge *et al.*, 2019). We made use of the merged assembly to explore the fully assembled 64.1 Mbp introgression from *S. peruvianum* where the *Tm-2*^{2} gene, conferring resistance to ToMV and TMV, resides.

Multiple technical developments have facilitated this highly contiguous tomato genome assembly. Firstly, HiFi reads are highly accurate and downsampling revealed that for inbred tomato as low as 20.3 Gbp (equal to about 24x coverage of our final merged assembly) was sufficient for an assembly with an N50 of 20.8 Mbp, with a largest contig of 66.3 Mbp (Supplementary Table 1). Secondly, HMW DNA extraction coupled with Circulomics long read enrichment can now reliably lead to ONT PromethION yields of at least 80 Gbp of usable data, with mean read lengths of at least 20 kbp. The longer ONT reads can facilitate assemblies with more complete chromosomes (Supplementary Fig. 1), yet gene completeness was slightly lower likely due to higher remaining uncorrectable base errors (Table 2). Thirdly, both HiFi and ONT assembly tools are now computationally efficient and allow the testing of various parameters and input data sets. Our HiFi data was assembled by Hifiasm in less than 2 hours with 128 threads, while Flye offers a fast but not as contiguous choice for the ONT platform. Even when using the NECAT assembler, it only takes 3 days with 256 threads to assemble a tomato genome. Finally, by merging the HiFi and ONT assemblies, which had different breakpoints, we were able to harness the complementarity of the two technologies. A recent comparison pointed out that PacBio HiFi reads tend to lead to better assembly of the barley genome than ONT (Mascher *et al.*, 2021), while here we showed how the complementarity of the two platforms can be leveraged. Highly accurate HiFi reads, and the longer, less accurate, ONT reads facilitated an assembly that spans many complex repeated sequences. For instance, PacBio HiFi read coverage dropped rapidly at several AT rich sequences which was complemented by ONT reads and ONT assembly tools (Supplementary Fig. 5a-c). The reduced coverage is potentially due to a “heat kill” step, which AT-rich sequences may be particularly sensitive to due to annealing properties, during HiFi library preparation (to destroy ligase enzyme) and is no longer recommended in the latest protocols. Here, we also found lower HiFi coverage in a CT/GA-rich region (Supplementary Fig. 5d), as has also been reported in the human genome (Nurk *et al.*, 2021), and its source remains to be identified. As in recent human, Arabidopsis and banana genome assemblies (Naish *et al.*, 2021; Nurk *et al.*, 2021; Belser *et al.*, 2021), the 5S rDNA and 45s rDNA sequences were not complete in our assembly, while some tomato centromeres and telomeres appear to be complete, including a convincing telomere-to-telomere (Hifiasm) assembly of chromosome 5 (Supplementary Fig. 6). Both technologies yielded assemblies that would have been impossible just two years ago, and it appears likely that higher quality ONT long read data (through new pore types and basecalling approaches) and longer HiFi reads (through new polymerase types) will further improve assembly metrics in the future. The approach we have used here may be used as a simple recipe in other similar sized, homozygous, genomes.

The *Tm-2*^{2} gene was known to be within a large introgression (Lin *et al.*, 2014) but the complete structure of the region has until now remained unassembled. Despite almost six decades of breeding, and passing through likely hundreds of backcrosses, there remains absolute linkage between the *Tm-2*^{2} gene and the two extremes of the introgression - a classic case of linkage drag (Fig. 4b & 4d) (Pelham, 1966; Lin *et al.*, 2014; Schouten *et al.*, 2019). The introgression in Moneyberg-TMV and Moneymaker-TMV is exactly the same length, agreeing with primary accounts of introgression history (see Materials and Methods), while the commercial hybrid Merlice, surprisingly, has a slightly longer introgression (Fig. 3d). The introgression contains several large inversions but the *Tm-2*^{2} gene itself is found in a region syntenic to *S. lycopersicum* (Fig. 3 a-c). Pericentromeric heterochromatin makes up about 70% of the tomato genome and meiotic crossovers rarely occur within these regions (De Haas *et al.*, 2017; Demirci *et al.*, 2017; Lhuissier *et al.*, 2007). The *Tm-2*^{2} gene is located within the pericentromeric heterochromatin and that region does not recombine in a Moneymaker x *S. pimpinellifolium* RIL population (where no *Tm-2*^{2} gene introgression is present), suggesting that the *Tm-2*^{2} gene position on chromosome 9 pre-disposes it to linkage drag. However, in the same RIL population crossovers do occur up to ~1.9 Mbp proximal of the start of the introgression (De Haas *et al.*, 2017). This suggests that the higher polymorphism rate and structural variation between *S. lycopersicum* and *S. peruvianum* (compared to the more closely related *S. lycopersicum* and *S. pimpinellifolium)* likely partially explain the extreme linkage drag in this region.

Why do meiotic crossovers not occur within regions of the introgression that are syntenic to *S. lycopersicum*? It remains to be determined whether meiotic DNA double strand breaks (DSBs), a prerequisite for crossovers, occur within the introgression and whether in hybrids that are hemizygous for the introgression chromosome 9 can completely synapse. Given that the introgression contains many genes, and gene promoters/terminators are targets for meiotic DSBs in plants (Choi *et al.*, 2018) it is probable that meiotic DSBs do occur within the introgression region, even in hemizygous hybrids. DSBs inside the introgression are likely repaired as non-crossovers. It is possible that the modulation of factors that can change chromosomal distributions of meiotic crossover (e.g. non-CG DNA methylation) could open up this region to meiotic recombination (Zhao *et al.*, 2021; Underwood *et al.*, 2018; Wang *et al.*, 2021).

Introgression of resistance genes from wild crop relatives can have negative side effects, such as reduced yield and quality, due to linkage drag (Chitwood-Brown *et al.*, 2021; Rubio *et al.*, 2016; Tanksley *et al.*, 1998). Employing the *Tm-2*^{2} gene introgression in a hemizygous state leads to a higher yield in field tomatoes (Tanksley *et al.*, 1998). However, marker studies and ONT-based comprehensive haplotyping showed that only two of the six commercial hybrids we studied employ the introgression in a hemizygous state (Fig. 4b & 4d) (Schouten *et al.*, 2019), which may be due to smaller yield gains of a hemizygous introgression in greenhouse varieties or to reduce the risk of ToMV/TMV infection during the production of hybrid seeds. Nonetheless, the *Tm-2*^{2} gene introgression from *S. peruvianum* alters the levels of more than three hundred metabolites (Zhu *et al.*, 2018), suggesting factors linked to the *Tm-2*^{2} gene compromise multiple important tomato traits. We expect that the rapid generation of near complete genome assemblies will be exploited in future to decode additional introgressions from wild crop relatives, and subsequent genome engineering will lead to resistant crop varieties with better yield and taste.

Materials and Methods

Plant materials and growth

Moneyberg-TMV was originally developed at De Ruiter seeds (Bleiswijk, South Holland, Netherlands) by introgression of the *Tm-2*^{2} gene from a source that contained *S. peruvianum* germplasm originally provided by Alexander (Alexander 1963). The *S. lycopersium* basis of the line originates from the Moneyberg cultivar, an open pollinated, indeterminate, greenhouse tomato cultivar, that was developed by selection from Moneymaker at Vandenberg seeds (Gebr. van den Berg, Naaldwijk, South Holland, Netherlands). Moneymaker itself was first developed in the early 1900s by Fred Stonor (Southampton, England, UK). Maxeza F1 (Truss tomato) and Tomagino F1 (Cherry tomato) were produced by Enza Zaden. Funtelle F1 (Date tomato) and Growdena F1 (Beefsteak tomato) were produced by Syngenta. Sevance F1 ("on the vine" tomato) and Merlice F1 (Truss tomato) were produced by De Ruiter seeds. Moneymaker-TMV seeds were from the stocks of WUR-Plant breeding which were originally provided by De Ruiter seeds. For further seed origin information please see the acknowledgements.

For genome sequencing and meiotic cytology, ten Moneyberg-TMV plants (all progeny of a single highly-inbred parent) were grown in the MPIPZ greenhouses during the late spring of 2020 under natural light supplemented with artificial light to ensure 16 hours light per day. Young unexpanded leaves were collected from 5-week-old plants and snap frozen in liquid nitrogen before interim storage at -80 degrees. For whole-genome resequencing, Moneymaker-TMV and Merlice plants were grown in the greenhouses of WUR until the third full leaf, and shoot tips with young leaves were harvested and snap frozen in liquid nitrogen. For marker studies, Moneyberg-TMV, LYC1969, Microtom, Heinz1706, Maxeza, Tomagino, Funtelle, Growdena and Sevance seeds were germinated *in vitro* on 0.8% agarose.

Chromosome spreading

Appropriate stages (3-4mm) of meiotic buds from Moneyberg-TMV were fixed in 1mL fresh Carnoy's solution composed of 3:1 (v/v) absolute ethanol:glacial acetic acid, and placed under vacuum for at least 30 minutes to ensure tissue infiltration. The Carnoy's solution was replaced and the samples kept at room temperature for 48 hours until they turned white. The fixed materials were used for chromosome spreading essentially as previously described (Ross *et al.*, 1996). In brief, 50-60 meiotic anthers were isolated from meiotic buds and placed into a 50 µL enzyme mixture (0.3% cellulase, 0.3% cytohelicase and 0.3% pectolyase in citric buffer 10 mM, pH 4.6) to digest for 2.5 hours at 37 °C. 2-3 anthers were used to make a single slide. After drying 8 µL DAPI (2 µg/mL) was added to stain the chromosomes. Finally, meiocytes images were taken using a Zeiss Axio Imager Z2 Microscope and images were analysed using the Zeiss ZEN 2 (blue edition) software.

Moneyberg-TMV High molecular weight DNA extraction

High molecular weight (HMW) DNA of Moneyberg-TMV was isolated from 1.5 grams of young leaf material with a NucleoBond HMW DNA kit (Macherey Nagel). DNA quality was assessed with a FEMTOpulse device (Agilent) and quantity measured using a Quantus Fluorometer (Promega).

Moneyberg-TMV Library preparations and sequencing

A HiFi library was prepared according to the manual "Procedure & Checklist - Preparing HiFi SMRTbell® Libraries using SMRTbell Express Template Prep Kit 2.0" with an initial DNA fragmentation by g-Tubes (Covaris) and final library size binning into defined fractions by SageELF (Sage Science). Size distribution was again controlled by FEMTOpulse (Agilent). Size-selected libraries with an expected insert size of 15 kbp and 18 kbp were independently sequenced on single SMRT cells of a Pacific Biosciences Sequel II device at the MPGC Cologne with Binding kit 2.0 and Sequel II Sequencing Kit 2.0 for 30 h (Pacific Biosciences).

9 µg of HMW DNA was size selected using the Circulomics Short-Read Eliminator XL Kit (Circulomics Cat# SKU SS-100-111-01). Out of this size selected DNA 1.5 µg was used as input for two library preparations with the Oxford Nanopore LSK-110 ligation sequencing Kit. Half of each library was loaded onto a PromethION FLO-PRO002 flowcell (R9.4.1 pores) and sequenced for 24 h. Then the flowcells were rinsed using the Oxford Nanopore Wash Kit WSH-003 and the second part of each library was loaded and sequencing continued for another 48 h. ONT sequencing was performed on an Oxford Nanopore P24 PromethION at the Forschungszentrum Jülich using MinKNOW version 21.02.7 without live basecalling. Basecalling of the Oxford Nanopore read data was done using guppy basecaller version 5.0.11 using the R9.4.1 PromethION super high-accuracy model (dna_r9.4.1_450bps_sup_prom) including filtering out basecalled reads with an average Phred-Score of less than 9.0. Reads with a Q-value below 9 were excluded before further analysis, including genome assembly. To remove adapter sequences and split chimeric reads the remaining Nanopore reads were then filtered further with porechop version 0.2.4 with default settings.

A chromatin conformation capture library was prepared using 0.5 grams of young leaf material as the input. All treatments were according to the recommendations of the kit vendor (Omni-C, Dovetail) for plants. As a final step, an Illumina-compatible library was prepared (Dovetail) with an insert size of 540bp and sequenced (paired-end 2 x 150 bp) on an Illumina NovaSeq 6000 at Novogene to generate 148.54 million PE reads.

Whole genome re-sequencing

Moneymaker-TMV and Merlice plant material was ground into fine powder by mortar and pestle, and DNA was isolated by a CTAB based method (Healey *et al.*, 2014). DNA was dissolved in ultrapure water and DNA was checked by gel, Qubit and nanodrop. Library preparation and whole genome sequencing was performed by Novogene using an Illumina device.

Genome assemblies and assembly statistics

Hifiasm v0.14.2 (Cheng *et al.*, 2021) used to assemble the HiFi reads with default settings. Canu v2.1.1 was used to assemble the HiFi reads in "HiCanu" mode (Nurk *et al.*, 2020) with an estimated genome size of 916 Mbp based on kmer counting of the raw HiFi data using Jellyfish v2.2.6 (Marçais and Kingsford, 2011).

Flye v2.8.2 (Kolmogorov *et al.*, 2019) was used to assemble the ONT reads with the option --nano-raw for unpolished Nanopore reads. NECAT version 0.0.1_update20200803 was used to assemble the ONT reads (Chen *et al.*, 2021) with default options apart from increasing the coverage used for assembly from 30x to 40x by setting PREP_OUTPUT_COVERAGE to 40.

ONT and HiFi reads were randomly subsampled in 9 sets of 90, 80, 70, 60, 50, 40, 30, 20 and 10% of the original reads and used for assemblies using NECAT (ONT) and Hifiasm (HiFi) with the same settings as for the original assemblies.

Quast v5.0.2 (Mikheenko *et al.*, 2018) and GAAS v1.1.0 (https://github.com/NBISweden/GAAS) were used to calculate statistics on fasta files. Benchmarking Universal Single Copy Orthologs (BUSCO) was calculated using BUSCO v5.2.1 (Seppey *et al.*, 2019) depending on hmmsearch v3.1 and metaeuk v4.a0f584d, was used with lineage datasets solanales (https://busco-data.ezlab.org/v5/data/lineages/solanales_odb10.2020-08-05.tar.gz) and eudicots (https://busco-data.ezlab.org/v5/data/lineages/eudicots_odb10.2020-09-10.tar.gz) to obtain evolutionarily-informed expectations of gene content. To assess the LTR assembly index (LAI) LTR retriever v2.9.0 (Ou *et al.*, 2018) was run with default settings on the respective genome assemblies.

MbTMV assembly pipeline

The NECAT assembly was polished with all of the ONT reads using Medaka v1.2.3 (https://nanoporetech.github.io/medaka/) and the model specific for PromethION R.9.4.1 data basecalled with guppy 5.0.11 in "super high accuracy" mode. The Flye assembly was also polished as described above.

Next, the NECAT 40x medaka and Flye v2.8.2 medaka assemblies were merged. This was done by running nucmer (part of mummer v.4.0.0rc1) with the -l parameter to prevent invalid contig links using the NECAT assembly as query and the Flye assembly as reference. The alignment table was then filtered with delta-filter (also part of mummer) using the options -r -q -i 0.95 to only use reciprocal best matches per region and a minimum identity of 95% in overlaps. This matches the default settings in the quickmerge wrapper which still relies on mummer version 3. Finally quickmerge (Chakraborty *et al.*, 2016) was used with the parameter -c 7.0 to increase stringency of merging regions to prevent assembly artifacts. The other parameters mandatory for quickmerge were set to the same values as used in the wrapper script by default (-hco 5.0 -l 0 -ml 5000). The resulting merged assembly was subsequently polished with all HiFi reads using Racon v1.4.3 (Vaser *et al.*, 2017) together with Minimap version 2.21 (Li, 2018) using the "map-hifi" preset for mapping the reads to the genome to overcome uncorrectable errors resulting from Nanopore reads.

In parallel, the Canu and Hifiasm assemblies were merged using the Canu assembly as reference and the Hifiasm assembly as query with quickmerge (as above) but using the default -c parameter of 1.5. Due to the low baseline error rate of HiFi Reads no further polishing was done on these assemblies.

The resulting merged (and polished) assemblies were then merged again using the Nanopore (Flye+NECAT) as query and the PacBio (Hifiasm+Canu) as reference using the same default parameters as for merging the two PacBio assemblies before. The final merged assembly was named MbTMV.

Dot plots

D-GENIES version 1.2.0 (Cabanettes and Klopp, 2018) was run with default settings with alignments generated using Minimap2 v2.21 (Li, 2018) providing the *Solanum lycopersicum* cv. 'Heinz1706' SL4.0 (Hosmani *et al.*, 2019) as reference (target) and our assembly as query. For legibility the chromosome names in both assemblies were shortened to "ch00 - ch12". Local installations of reDOTable v1.1 (https://www.bioinformatics.babraham.ac.uk/projects/redotable/ or github https://github.com/s-andrews/redotable) were used to generate dotplots.

Validation of MbTMV assembly

Following the esrice/hic-pipeline (https://github.com/esrice/hic-pipeline), Omni-C (Dovetail) paired end reads were mapped separately using Burrows-Wheeler Aligner v0.7 (Li and Durbin, 2009) and the filter_chimeras.py script. Mapped reads were combined using the combine_ends.py script, with 3 iteration steps and a minimum mapping quality value of 20 (default), followed by adding read mate scores, sorting and removing duplicate reads using Samtools v1.9 (Danecek *et al.*, 2021). The resulting bam file was converted to a bed file and sorted (-k 4) using Bedtools v2.30 (Quinlan and Hall, 2010). We ran one single round of Salsa v2.2 (Ghurye *et al.*, 2019) with optional settings: -e DNASE -m yes -p yes.

A modified version of the convert.sh script was used to convert the Salsa2 output to a Hi-C file, which was used within a local installation Juicebox (https://github.com/aidenlab/Juicebox) v1.11.08 to generate a Hi-C contact plot.

The MbTMV genome assembly was aligned to SL4.0 (Hosmani *et al.*, 2019) using Minimap2 v2.17 (Li, 2018) with default settings, followed by running RaGOO v1.11 (Alonge *et al.*, 2019) with default options.

Coverage analysis and circos plot of MbTMV assembly

ONT data was mapped using Minimap2 version 2.18-r1028-dirty (Li, 2018), with the preset "map-ont" whereas PacBio HiFi data was mapped with the preset "map-hifi". The output SAM file was converted, sorted and indexed using Samtools v1.9 (Danecek *et al.*, 2021). Samtools v1.9 (Danecek *et al.*, 2021) was used to extract the coverage per base, including positions with zero depth, from the bam file. The resulting average depth was summarized in overlapping windows of 200 kbp every 100 kbp and visualized using NG-circos (Cui *et al.*, 2020). In addition, sequences of the 45S rDNA intergenic spacer, 5S rDNA, 45S rDNA, telomeric repeat and TGR1-4 were searched in MbTMV using blastn and counted in non-overlapping windows of size 1 Mbp.

For coverage plot in Supp figure 3: PacBio HiFi data was mapped to the MbTMV genome assembly using pbmm2 (version 1.4.0) with the preset "CCS" (https://github.com/PacificBiosciences/pbbioconda). ONT data was mapped to the MbTMV genome using Minimap2 version 2.17 (Li, 2018) with the preset "map-ont" and "eqx", followed by converting, sorting and indexing of the output file using Samtools v1.9 (Danecek *et al.*, 2021). Read coverage was extracted in 100kb windows using Mosdepth (Pedersen and Quinlan, 2018) and plotted in the middle of each interval within R version 4.0.3 (2020-10-10) (https://cran.r-project.org/) using ggplot2 and the tidyverse package (https://www.tidyverse.org/).
For Supp figure 5: PacBio HiFi, ONT and ONT-NECAT read coverage was visualized using a local installation of IGV (v2.8.13) (Robinson *et al.*, 2011).

Genome alignment, SV detection and further genome analysis

Genomes were aligned to SL4.0 (Hosmani *et al.*, 2019), using Minimap2 v2.17 (Li, 2018) with options -ax asm5 --eqx, followed by running SyRI v1.4 (Goel *et al.*, 2019), to identify and call polymorphisms and structural variations, with optional settings: -k -F S --log WARN. Plotsr v5 (Goel *et al.*, 2019) was used with options -B <annotation.bed> -H <1-9> and -W <1-9> to generate SyRI plots. Fasta headers of genomes were manually formatted to match between genomes, using sed command line, and chromosome 0 was removed, using awk command line, before aligning the genomes. Chromosome 1, 2, 7, 8 and 12 of the MbTMV assembly were reverse complemented before alignment, using cat command line.

Using the SyRI generated vcf output of the whole chromosome alignment (Supplementary Dataset 4), sequences used for Figures 3B and 3C were extracted (SL4.0:6286825-14549782 MbTMV:7314513-17630288 and SL4.0:13227892-14039189 MbTMV:15980168-17044082 for figure 3B and 3C, respectively), using Samtools v1.9 (Danecek *et al.*, 2021). Sequences were aligned using Minimap2 v2.17 (Li, 2018) with options -ax asm5 --eqx followed by running SyRI v1.4 and Plotsr v5 (Goel *et al.*, 2019). Figures 3B and 3C were manually edited using Adobe Illustrator 25.2.3 adding genomic positions based on extracted regions.

Chromosome lengths were extracted from the fasta files, MbTMV, *S. lycopersicum* cv. 'Heinz1706' SL4.0 (Hosmani *et al.*, 2019), obtained from ftp://ftp.solgenomics.net/genomes/Solanum_lycopersicum/Heinz1706/assembly/build_4.00/S_lycopersicum_chromosomes.4.00.fa, *S. pennellii* 'LA0716' (Bolger *et al.*, 2014), obtained from ftp://ftp.solgenomics.net/genomes/Solanum_pennellii/Spenn.fasta, *S. pimpinellifolium* 'LA2093' v1.5 (X., Wang *et al.*, 2020) obtained from ftp://ftp.solgenomics.net/genomes/Solanum_pimpinellifolium/LA2093/Spimp_LA2093_genome_v1.5/LA2093_genome_v1.5.fa, using awk command line and plotted within R version 4.0.3 using ggplot2 and the tidyverse package.

Further analysis of chromosome 9 introgression

M82 and LYC 1969 ONT data (Alonge *et al.*, 2020) were mapped to both SL4.0 and MbTMV using Minimap2 v2.17 (Li, 2018), with the options -ax map-ont --eqx. The output SAM file was converted, sorted and indexed using Samtools v1.9 (Danecek *et al.*, 2021). Coverage plots per chromosome were constructed with goleft IndexCov v0.2.4 (Pedersen *et al.*, 2017).

Moneymaker and Merlice illumina data was mapped to SL4.0 using bowtie2 v2.2.8 with options -q --phred33 --very-sensitive --no-unal -p 12 -x <SL4.0.fasta> -U reads1.fq,reads2.fq -S. Variant calling was done using bcftools v1.9 mpileup and call with options -mv -Ov (Li, 2011) (https://samtools.github.io/bcftools/bcftools.html).

SNP density was extracted from MbTMV (SyRi output), MoneymakerTMV and Merlice vcf files using VCFtools v.0.1.16 (Danecek *et al.*, 2011). Plots were made within R 4.0.3 (2020-10-10) (https://cran.r-project.org/) using ggplot2 and the tidyverse package (https://www.tidyverse.org/).

Marker studies

Cotyledons from *in vitro* germinated samples were collected and lyophilized overnight in an Alpha 1-4 freeze dryer (Martin Christ GmbH). DNA extraction was performed using the BioSprint 96 DNA Plant kit protocol (Qiagen) and eluted in 200μl AE buffer. M-1 was amplified using the primers dCUn0256 (GGAACCTCGAGTCCTTACAGT) and dCUn0257 (GGCAGCCATTAGCAAACCCA). M-TM2^2 was amplified using published primers (Lanfermeijer *et al.*, 2005). M-2 was amplified using the primers dCUn0258 (TTCTGTTCCAGACCCGACCT) and dCUn0259 (CCCATTAACCTCCAGACGGG). 35 rounds of PCR were performed using Mango Taq (Bioline) under standard conditions. M-1 was digested with AflII (NEB) overnight at 37°C, M-TM2^2 was digested with BslI (NEB) for 3 hours at 55°C and M-2 was digested with XhoI (NEB) overnight at 37°C. 10µl per restriction digest was loaded on a 3% agarose gel.

Funtelle F$_1$ hybrid sequencing, genome assembly and analysis

DNA from the hybrid *S. lycopersicum* cv. ‘Funtelle’ was extracted using the Machery Nagel Nucleobond HMW DNA Kit. HMW DNA was size selected using the Circulomics Short-Read Eliminator XL Kit (Circulomics Cat# SKU SS-100-111-01) and used as input for library preparation with the Oxford Nanopore LSK-110 ligation sequencing Kit. Four libraries from the same sample were loaded onto three PromethION FLO-PRO002 flowcells and one MinION flowcell (all R9.4.1 pores) and sequenced. ONT sequencing was performed on an Oxford Nanopore P24 PromethION and a MinION MK1B at the Forschungszentrum Jülich using MinKNOW version 21.02.7 without live basecalling. Basecalling of the Oxford Nanopore read data was done using guppy basecaller version 5.0.11 using the R9.4.1 PromethION super-high-accuracy model (dna_r9.4.1_450bps_sup_prom) and the R9.4.1 MinION super-high-accuracy model (dna_r9.4.1_450bps_sup). ONT reads were assembled with Flye v2.8.2 using the same settings as for ‘Moneyberg-TMV’. The contigs from the Flye assembly of ‘Funtelle’ were separately aligned against the MbTMV and SL4.0 assemblies using Minimap2 v2.21 and the alignments were interrogated using D-GENIES version 1.2.0 (default settings). All contigs that aligned to Chr9^{MbTMV} or Chr9$^{SL4.0}$ were extracted and competitively realigned using Minimap2 v2.21 to a Fasta file containing both Chr9^{MbTMV} and Chr9$^{SL4.0}$, and the alignment was visualized using D-GENIES version 1.2.0 (default settings).

Data availability

PacBio HiFi consensus reads (Moneyberg-TMV), ONT sequencing reads (Moneyberg-TMV), OmniC Illumina reads (Moneyberg-TMV) and the MbTMV genome assembly were deposited in the EMBL-EBI European Nucleotide Archive under project number PRJEB44956. ONT sequencing reads for Funtelle and Illumina reads for Moneymaker-TMV and Merlice are also deposited under the same accession code. The Flye genome assembly from Funtelle ONT reads is made available at Dryad (https://doi.org/10.5061/dryad.3j9kd51kn).

Acknowledgements

Moneyberg-TMV seeds were kindly provided for research purposes by Cilia Lelivelt and Maarten Verlaan (Rijk Zwaan, Netherlands). Maxeza F$_1$ and Tomagino F$_1$ tomato seeds were kindly provided for research purposes by Martijn van Stee (Enza Zaden, Netherlands). Funtelle F$_1$ and Growdena F$_1$ tomato seeds were kindly provided for research purposes by Axel Voss (Syngenta, Germany). Sevance F$_1$ seeds (De Ruiter seeds, part of Bayer Group) were purchased for research purposes from Volmary GmbH (Münster, Germany). Merlice F$_1$ seeds (De Ruiter seeds, part of Bayer Group) were provided by Tomato World (Netherlands) to HJS for research purposes. Microtom seeds were originally sourced from the Tomato Growers Supply company (Ft. Myers, Florida, USA). LYC1969 seeds were a gift from Zachary Lippman (CSHL, USA). Heinz 1706 seeds were provided by the Centre for Genetic Resources (Wageningen, Netherlands). We are grateful to Gerard Bijsterbosch (WUR) for isolating DNA from Moneymaker-TMV and Merlice. We thank Saurabh Pophaly (MPIPZ), Manish Goel (MPIPZ) and Danny Esselink (WUR) for assistance with bioinformatic analysis. We thank Korbinian Schneeberger (MPIPZ), Quentin Gouil (Walter and Eliza Hall Institute) and Alex Canto-Pastor (UC Davis) for comments on the manuscript. Information on the breeding history of Moneymaker, Moneyberg and Moneyberg-TMV varieties was kindly provided by Theo Schotte (Solynta, Netherlands) and Maarten Koornneef (WUR/MPIPZ). This work was supported by the Max Planck Society, a PhD fellowship awarded to M. W. A. M. Z. from the Malaysian Agricultural Research and Development Institute (MARDI), grants awarded to B. U. (DFG US 98/23, CEPLAS EXC2048 and BMBF 031A536C) and the WUR Department of Plant Breeding (H.S.). This manuscript is dedicated to Eric Robinson Smith whose favourite tomato variety was Moneymaker.

Author contributions

WMJR and SE cultivated and collected plant materials. BH performed DNA extractions and HiFi sequencing. MHWS and DBL performed DNA extractions and ONT sequencing. MHWS, WMJR and DBL performed genome assemblies. MHWS performed downsampling analysis and assembly merging. WMJR performed validation of the merged assembly and the majority of the downstream bioinformatic analysis with contributions from MHWS. YW performed chromosome spreading experiments. HJS contributed Illumina sequencing data for Moneymaker-TMV and Merlice. All authors contributed to the analysis and interpretation of data. WMJR generated main and supplementary figures with contributions from MWHS, BU and CJU. CJU coordinated the project. WMJR, MWHS, BU and CJU wrote the manuscript with comments from all other authors.

Conflicts of interests

The authors declare that they have no competing interests.

Supporting information

Supplementary Fig. 1. Alignment of four Moneyberg-TMV genome assemblies with Heinz 1706 (SL4.0) assembly

Supplementary Fig. 2. Alignment of the merged assemblies to SL4.0

Supplementary Fig. 3. PacBio HiFi and ONT coverage plots

Supplementary Fig. 4. Dotplot of self-alignment of repetitive regions on MbTMV chromosomes 1 and 2

Supplementary Fig. 5. Examples of complementary sequencing data visualized in IGV

Supplementary Fig. 6. Synteny plots of different chromosome 5 assemblies

Supplementary Fig. 7. SNP frequency plot between MbTMV and SL4.0 in 10 kbp windows along chromosome 9

Supplementary Fig. 8. Coverage plot of LYC1969 and M82 ONT reads aligned to MbTMV chromosome 9 and SL4.0 chromosome 9

Supplementary Fig. 9. Agarose gel image of molecular marker analysis

Supplementary Table 1) Downsampling of PacBio HiFi reads and assembly using Hifiasm

Supplementary Table 2) Downsampling of ONT reads and assembly using NECAT

Supplementary Table 3) Transition points of the MbTMV assembly

Supplementary Table 4) Classification of unplaced contigs in the MbTMV assembly

Supplementary Table 5) Statistics of MbTMV assembly and RaGOO output

Dataset S1) PAF files showing the approximate mapping positions between SL4.0 and non-merged Moneyberg-TMV assemblies

Dataset S2) PAF files showing the approximate mapping positions between SL4.0 and merged Moneyberg-TMV assemblies

Dataset S3) SyRI called variants between MbTMV chromosome 9 and SL4.0 chromosome 9, extracted from the whole genome alignment

Dataset S4) SyRI called variants between MbTMV chromosome 9 and SL4.0 chromosome 9, from a direct alignment of MbTMV chromosome 9 and SL4.0 chromosome 9

Dataset S5) SyRI called variants between MbTMV chromosome 9 and SL4.0 chromosome 9, from a ~10Mb extracted region

Dataset S6) SyRI called variants between MbTMV chromosome 9 and SL4.0 chromosome 9, from a ~1Mb extracted region

References

Aflitos, S., Schijlen, E., Jong, H. de, et al. (2014) Exploring genetic variation in the tomato (*Solanum* section *Lycopersicon*) clade by whole-genome sequencing. *Plant J.*, **80**, 136–148. Available at: http://www.ncbi.nlm.nih.gov/pubmed/25039268 [Accessed December 3, 2018].

Alexander, L.J. (1963) Transfer of a dominant type of resistance to the four known Ohio pathogenic strains of tobacco mosaic virus (TMV) from Lycopersicon peruvianum to L. esculentum. *Phytopathology*, **53**, 896.

Alonge, M., Soyk, S., Ramakrishnan, S., Wang, X., Goodwin, S., Sedlazeck, F.J., Lippman, Z.B. and Schatz, M.C. (2019) RaGOO: fast and accurate reference-guided scaffolding of draft genomes. *Genome Biol. 2019 201*, **20**, 1–17. Available at: https://genomebiology.biomedcentral.com/articles/10.1186/s13059-019-1829-6 [Accessed August 19, 2021].

Alonge, M., Wang, X., Benoit, M., et al. (2020) Major Impacts of Widespread Structural Variation on Gene Expression and Crop Improvement in Tomato. *Cell*, **182**, 145-161.e23.

Bai, Y. and Lindhout, P. (2007) Domestication and breeding of tomatoes: What have we gained and what can we gain in the future? *Ann. Bot.*, **100**, 1085–1094. Available at: /pmc/articles/PMC2759208/ [Accessed April 30, 2021].

Belser, C., Baurens, F.-C., Noel, B., et al. (2021) Telomere-to-telomere gapless chromosomes of banana using nanopore sequencing. *bioRxiv*, 2021.04.16.440017. Available at: https://www.biorxiv.org/content/10.1101/2021.04.16.440017v1 [Accessed August 19, 2021].

Berlin, K., Koren, S., Chin, C.S., Drake, J.P., Landolin, J.M. and Phillippy, A.M. (2015) Assembling large genomes with single-molecule sequencing and locality-sensitive hashing. *Nat. Biotechnol.*, **33**, 623–630. Available at: https://www.nature.com/articles/nbt.3238 [Accessed July 4, 2021].

Bolger, A., Scossa, F., Bolger, M.E., et al. (2014) The genome of the stress-tolerant wild tomato species Solanum pennellii. *Nat. Genet.*, **46**, 1034–1038. Available at: http://www.nature.com/articles/ng.3046 [Accessed December 16, 2018].

Cabanettes, F. and Klopp, C. (2018) D-GENIES: dot plot large genomes in an interactive, efficient and simple way. *PeerJ*, **6**, e4958. Available at: https://peerj.com/articles/4958 [Accessed August 19, 2021].

Chakraborty, M., Baldwin-Brown, J.G., Long, A.D. and Emerson, J.J. (2016) Contiguous and accurate de novo assembly of metazoan genomes with modest long read coverage. *Nucleic Acids Res.*, **44**, e147. Available at: /pmc/articles/PMC5100563/ [Accessed August 19, 2021].

Chang, S. Bin, Yang, T.J., Datema, E., et al. (2008) FISH mapping and molecular organization of the major repetitive sequences of tomato. *Chromosom. Res.*, **16**, 919–933. Available at: http://www.sgn.cornell.edu/; [Accessed July 4, 2021].

Chen, Y., Nie, F., Xie, S.-Q., et al. (2021) Efficient assembly of nanopore reads via highly accurate and intact error correction. *Nat. Commun. 2021 121*, **12**, 1–10. Available at: https://www.nature.com/articles/s41467-020-20236-7 [Accessed August 19, 2021].

Cheng, H., Concepcion, G.T., Feng, X., Zhang, H. and Li, H. (2021) Haplotyperesolved de novo assembly using phased assembly graphs with hifiasm. *Nat. Methods 2021 182*, **18**, 170–175. Available at: https://www.nature.com/articles/s41592-020-01056-5 [Accessed August 19, 2021].

Chitwood-Brown, J., Vallad, G.E., Lee, T.G. and Hutton, S.F. (2021) Characterization and elimination of linkage-drag associated with Fusarium wilt race 3 resistance genes. *Theor. Appl. Genet.*, **1**, 3. Available at: https://doi.org/10.1007/s00122-021-03810-5 [Accessed July 4, 2021].

Choi, K., Zhao, X., Tock, A.J., et al. (2018) Nucleosomes and DNA methylation shape meiotic DSB frequency in Arabidopsis thaliana transposons and gene regulatory regions. *Genome Res.*, **28**, 532–546. Available at: http://www.ncbi.nlm.nih.gov/pubmed/29530928 [Accessed November 23, 2018].

Costa, J.M. and Heuvelink, E. (2018) The global tomato industry. In *Tomatoes*. CABI, pp. 1–26.

Cui, Y., Cui, Z., Xu, J., et al. (2020) NG-Circos: next-generation Circos for data visualization and interpretation. *NAR Genomics Bioinforma.*, **2**. Available at: https://academic.oup.com/nargab/article/2/3/lqaa069/5901067 [Accessed August 19, 2021].

Danecek, P., Auton, A., Abecasis, G., et al. (2011) The variant call format and VCFtools. *Bioinformatics*, **27**, 2156–2158. Available at: https://academic.oup.com/bioinformatics/article/27/15/2156/402296 [Accessed August 19, 2021].

Danecek, P., Bonfield, J.K., Liddle, J., et al. (2021) Twelve years of SAMtools and BCFtools. *Gigascience*, **10**, 1–4. Available at: https://academic.oup.com/gigascience/article/10/2/giab008/6137722 [Accessed August 19, 2021].

Demirci, S., Dijk, A.D.J. van, Sanchez Perez, G., Aflitos, S.A., Ridder, D. de and Peters, S.A. (2017) Distribution, position and genomic characteristics of crossovers in tomato recombinant inbred lines derived from an interspecific cross between *Solanum lycopersicum* and *Solanum pimpinellifolium*. *Plant J.*, **89**, 554–564.

Dumschott, K., Schmidt, M.H.W., Chawla, H.S., Snowdon, R. and Usadel, B. (2020) Oxford Nanopore sequencing: new opportunities for plant genomics? *J. Exp. Bot.*, **71**, 5313–5322. Available at: http://jxb.oxfordjournals.org/open_access.html [Accessed July 4, 2021].

Foolad, M.R., Stoltz, T., Dervinis, C., Rodriguez, R.L. and Jones, R.A. (1997) Mapping QTLs conferring salt tolerance during germination in tomato by selective genotyping. *Mol. Breed.*, **3**, 269–277. Available at: https://link.springer.com/article/10.1023/A:1009668325331 [Accessed August 24, 2021].

Ganal, M.W., Lapitan, N.L. and Tanksley, S.D. (1991) Macrostructure of the tomato telomeres. *Plant Cell*, **3**, 87–94. Available at: https://academic.oup.com/plcell/article/3/1/87/5984286 [Accessed August 19, 2021].

Gao, L., Gonda, I., Sun, H., et al. (2019) The tomato pan-genome uncovers new genes and a rare allele regulating fruit flavor. *Nat. Genet.*, **51**, 1044–1051. Available at: https://doi.org/10.1038/s41588-019-0410-2 [Accessed July 4, 2021].

Ghurye, J., Rhie, A., Walenz, B.P., Schmitt, A., Selvaraj, S., Pop, M., Phillippy, A.M.

and Koren, S. (2019) Integrating Hi-C links with assembly graphs for chromosome-scale assembly. *PLOS Comput. Biol.*, **15**, e1007273. Available at: https://journals.plos.org/ploscompbiol/article?id=10.1371/journal.pcbi.1007273 [Accessed August 19, 2021].

Goel, M., Sun, H., Jiao, W.B. and Schneeberger, K. (2019) SyRI: finding genomic rearrangements and local sequence differences from whole-genome assemblies. *Genome Biol.*, **20**, 1–13. Available at: https://doi.org/10.1186/s13059-019-1911-0 [Accessed July 4, 2021].

Haas, L.S. De, Koopmans, R., Lelivelt, C.L.C., Ursem, R., Dirks, R. and James, G.V. (2017) Low-coverage resequencing detectsmeiotic recombination pattern and features in tomato RILs. *DNA Res.*, **24**, 549–558. Available at: https://academic.oup.com/dnaresearch/article-lookup/doi/10.1093/dnares/dsx024 [Accessed November 19, 2017].

Healey, A., Furtado, A., Cooper, T. and Henry, R.J. (2014) Protocol: a simple method for extracting next-generation sequencing quality genomic DNA from recalcitrant plant species. *Plant Methods 2014 101*, **10**, 1–8. Available at: https://plantmethods.biomedcentral.com/articles/10.1186/1746-4811-10-21 [Accessed August 19, 2021].

Hon, T., Mars, K., Young, G., et al. (2020) Highly accurate long-read HiFi sequencing data for five complex genomes. *Sci. Data*, **7**, 1–11. Available at: https://www.nature.com/articles/s41597-020-00743-4 [Accessed August 30, 2021].

Hosmani, P., Flores-Gonzalez, M., Geest, H. van de, et al. (2019) An improved de novo assembly and annotation of the tomato reference genome using single-molecule sequencing, Hi-C proximity ligation and optical maps. *bioRxiv*, 767764. Available at: https://doi.org/10.1101/767764 [Accessed July 4, 2021].

Jo, S.-H., Koo, D.-H., Kim, J.F., Hur, C.-G., Lee, S., Yang, T., Kwon, S.-Y. and Choi, D. (2009) Evolution of ribosomal DNA-derived satellite repeat in tomato genome. *BMC Plant Biol.*, **9**, 42. Available at: /pmc/articles/PMC2679016/ [Accessed August 26, 2021].

Kim, H.T. and Lee, J.M. (2018) Organellar genome analysis reveals endosymbiotic gene transfers in tomato. *PLoS One*, **13**. Available at: https://pubmed.ncbi.nlm.nih.gov/30183712/ [Accessed August 29, 2021].

Kolmogorov, M., Yuan, J., Lin, Y. and Pevzner, P.A. (2019) Assembly of long, error-prone reads using repeat graphs. *Nat. Biotechnol.*, **37**, 540–546. Available at: https://www.nature.com/articles/s41587-019-0072-8 [Accessed August 19, 2021].

Koren, S., Schatz, M.C., Walenz, B.P., et al. (2012) Hybrid error correction and de novo assembly of single-molecule sequencing reads. *Nat. Biotechnol.*, **30**, 693–700. Available at: https://www.nature.com/articles/nbt.2280 [Accessed July 4, 2021].

Lanfermeijer, F.C., Dijkhuis, J., Sturre, M.J.G., Haan, P. De and Hille, J. (2003) Cloning and characterization of the durable tomato mosaic virus resistance gene Tm-22 from Lycopersicon esculentum. *Plant Mol. Biol.*, **52**, 1037–1049. Available at: https://link.springer.com/article/10.1023/A:1025434519282 [Accessed July 4, 2021].

Lanfermeijer, F.C., Warmink, J. and Hille, J. (2005) The products of the broken Tm-2 and the durable Tm-22 resistance genes from tomato differ in four amino acids. *J.*

Exp. Bot., **56**, 2925–2933. Available at: https://academic.oup.com/jxb/article/56/421/2925/593476 [Accessed July 4, 2021].

Lhuissier, F.G.P., Offenberg, H.H., Wittich, P.E., Vischer, N.O.E. and Heyting, C. (2007) The mismatch repair protein MLH1 marks a subset of strongly interfering crossovers in tomato. *Plant Cell*, **19**, 862–876. Available at: http://www.ncbi.nlm.nih.gov/pubmed/17337626 [Accessed December 13, 2018].

Li, H. (2011) A statistical framework for SNP calling, mutation discovery, association mapping and population genetical parameter estimation from sequencing data. *Bioinformatics*, **27**, 2987–2993. Available at: /pmc/articles/PMC3198575/ [Accessed August 30, 2021].

Li, H. (2018) Minimap2: Pairwise alignment for nucleotide sequences. *Bioinformatics*, **34**, 3094–3100.

Li, H. and Durbin, R. (2009) Fast and accurate short read alignment with Burrows-Wheeler transform. *Bioinformatics*, **25**, 1754–1760. Available at: https://pubmed.ncbi.nlm.nih.gov/19451168/ [Accessed November 11, 2020].

Li, J., Liu, L., Bai, Y., Zhang, P., Finkers, R., Du, Y., Visser, R.G.F. and Heusden, A.W. van (2010) Seedling salt tolerance in tomato. *Euphytica*, **178**, 403–414. Available at: https://link.springer.com/article/10.1007/s10681-010-0321-x [Accessed August 24, 2021].

Lin, T., Zhu, G., Zhang, J., et al. (2014) Genomic analyses provide insights into the history of tomato breeding. *Nat. Genet.*, **46**, 1220–1226. Available at: http://www.nature.com/articles/ng.3117 [Accessed December 3, 2018].

Liu, Y., Du, H., Li, P., et al. (2020) Pan-Genome of Wild and Cultivated Soybeans. *Cell*, **182**, 162-176.e13.

Marçais, G. and Kingsford, C. (2011) A fast, lock-free approach for efficient parallel counting of occurrences of k-mers. *Bioinformatics*, **27**, 764–770. Available at: https://academic.oup.com/bioinformatics/article/27/6/764/234905 [Accessed August 19, 2021].

Mascher, M., Wicker, T., Jenkins, J., et al. (2021) Long-read sequence assembly: a technical evaluation in barley. *Plant Cell*, **33**, 1888–1906. Available at: https://pubmed.ncbi.nlm.nih.gov/33710295/ [Accessed July 4, 2021].

Michael, T.P., Jupe, F., Bemm, F., Motley, S.T., Sandoval, J.P., Lanz, C., Loudet, O., Weigel, D. and Ecker, J.R. (2018) High contiguity Arabidopsis thaliana genome assembly with a single nanopore flow cell. *Nat. Commun.*, **9**, 1–8. Available at: www.nature.com/naturecommunications [Accessed July 4, 2021].

Mikheenko, A., Prjibelski, A., Saveliev, V., Antipov, D. and Gurevich, A. (2018) Versatile genome assembly evaluation with QUAST-LG. *Bioinformatics*, **34**, i142–i150. Available at: https://academic.oup.com/bioinformatics/article/34/13/i142/5045727 [Accessed August 19, 2021].

Naish, M., Alonge, M., Wlodzimierz, P., et al. (2021) The genetic and epigenetic landscape of the Arabidopsis centromeres. *bioRxiv*, 2021.05.30.446350. Available at: https://www.biorxiv.org/content/10.1101/2021.05.30.446350v2 [Accessed August 19, 2021].

Nurk, S., Koren, S., Rhie, A., et al. (2021) The complete sequence of a human genome. *bioRxiv*, 2021.05.26.445798. Available at:

https://www.biorxiv.org/content/10.1101/2021.05.26.445798v1 [Accessed August 19, 2021].

Nurk, S., Walenz, B.P., Rhie, A., et al. (2020) HiCanu: accurate assembly of segmental duplications, satellites, and allelic variants from high-fidelity long reads. *Genome Res.*, **30**, gr.263566.120. Available at: https://genome.cshlp.org/content/early/2020/08/14/gr.263566.120 [Accessed August 19, 2021].

Ou, S., Chen, J. and Jiang, N. (2018) Assessing genome assembly quality using the LTR Assembly Index (LAI). *Nucleic Acids Res.*, **46**, e126. Available at: https://github.com/oushujun/ [Accessed July 4, 2021].

Payne, A., Holmes, N., Rakyan, V. and Loose, M. (2019) Bulkvis: A graphical viewer for Oxford nanopore bulk FAST5 files. *Bioinformatics*, **35**, 2193–2198. Available at: https://pubmed.ncbi.nlm.nih.gov/30462145/ [Accessed August 26, 2021].

Pedersen, B.S., Collins, R.L., Talkowski, M.E. and Quinlan, A.R. (2017) Indexcov: Fast coverage quality control for whole-genome sequencing. *Gigascience*, **6**. Available at: https://pubmed.ncbi.nlm.nih.gov/29048539/ [Accessed August 19, 2021].

Pedersen, B.S. and Quinlan, A.R. (2018) Mosdepth: quick coverage calculation for genomes and exomes. *Bioinformatics*, **34**, 867–868. Available at: https://academic.oup.com/bioinformatics/article/34/5/867/4583630 [Accessed November 16, 2021].

Pelham, J. (1966) Resistance in tomato to tobacco mosaic virus. *Euphytica*, **15**, 258–267. Available at: https://link.springer.com/article/10.1007/BF00022331 [Accessed July 4, 2021].

Peralta, I.E., Spooner, D.M. and Knapp, S. (2008) *Taxonomy of wild tomatoes and their relatives (Solanum sect. Lycopersicoides, sect. Juglandifolia, sect. Lycopersicon ; Solanaceae)*, American Society of Plant Taxonomists. Available at: http://agris.fao.org/agris-search/search.do?recordID=US201300127979 [Accessed December 16, 2018].

Perry, K.L. and Palukaitis, P. (1990) Transcription of tomato ribosomal DNA and the organization of the intergenic spacer. *MGG Mol. Gen. Genet.*, **221**, 102–112. Available at: https://pubmed.ncbi.nlm.nih.gov/2325628/ [Accessed July 4, 2021].

Powell, A.F., Courtney, L.E., Schmidt, M.H.-W., et al. (2020) A Solanum lycopersicoides reference genome facilitates biological discovery in tomato. *bioRxiv*, 2020.04.16.039636.

Qin, P., Lu, H., Du, H., et al. (2021) Pan-genome analysis of 33 genetically diverse rice accessions reveals hidden genomic variations. *Cell*, **184**, 3542-3558.e16.

Quinlan, A. and Hall, I. (2010) BEDTools: a flexible suite of utilities for comparing genomic features. *Bioinformatics*, **26**, 841–842. Available at: https://pubmed.ncbi.nlm.nih.gov/20110278/ [Accessed August 19, 2021].

Robinson, J.T., Thorvaldsdóttir, H., Winckler, W., Guttman, M., Lander, E.S., Getz, G. and Mesirov, J.P. (2011) Integrative genomics viewer. *Nat. Biotechnol. 2011 291*, **29**, 24–26. Available at: https://www.nature.com/articles/nbt.1754 [Accessed November 16, 2021].

Ross, K.J., Fransz, P. and Jones, G.H. (1996) A light microscopic atlas of meiosis in Arabidopsis thaliana. *Chromosom. Res.*, **4**, 507–516. Available at:

https://link.springer.com/article/10.1007/BF02261778 [Accessed August 30, 2021].

Rubio, F., Alonso, A., García-Martínez, S. and Ruiz, J.J. (2016) Introgression of virus-resistance genes into traditional Spanish tomato cultivars (Solanum lycopersicum L.): Effects on yield and quality. *Sci. Hortic. (Amsterdam).*, **198**, 183–190.

Sato, S., Tabata, S., Hirakawa, H., et al. (2012) The tomato genome sequence provides insights into fleshy fruit evolution. *Nature*, **485**, 635–641. Available at: http://www.ncbi.nlm.nih.gov/pubmed/22660326 [Accessed November 27, 2017].

Schmidt-Puchta, W., Günther, I. and Sänger, H.L. (1989) Nucleotide sequence of the intergenic spacer (IGS) of the tomato ribosomal DNA. *Plant Mol. Biol.*, **13**, 251–253. Available at: https://link.springer.com/article/10.1007/BF00016143 [Accessed July 4, 2021].

Schmidt, M.H.W., Vogel, A., Denton, A.K., et al. (2017) De novo assembly of a new Solanum pennellii accession using nanopore sequencing. *Plant Cell*, **29**, 2336–2348.

Schouten, H.J., Tikunov, Y., Verkerke, W., Finkers, R., Bovy, A., Bai, Y. and Visser, R.G.F. (2019) Breeding Has Increased the Diversity of Cultivated Tomato in The Netherlands. *Front. Plant Sci.*, **10**, 1606. Available at: https://www.frontiersin.org/article/10.3389/fpls.2019.01606/full [Accessed May 15, 2020].

Seppey, M., Manni, M. and Zdobnov, E.M. (2019) BUSCO: Assessing Genome Assembly and Annotation Completeness. *Methods Mol. Biol.*, **1962**, 227–245. Available at: https://link.springer.com/protocol/10.1007/978-1-4939-9173-0_14 [Accessed August 19, 2021].

Simão, F.A., Waterhouse, R.M., Ioannidis, P., Kriventseva, E. V. and Zdobnov, E.M. (2015) BUSCO: assessing genome assembly and annotation completeness with single-copy orthologs. *Bioinformatics*, **31**, 3210–3212. Available at: https://pubmed.ncbi.nlm.nih.gov/26059717/ [Accessed November 17, 2021].

Tanksley, S.D., Bernachi, D., Beck-Bunn, T., et al. (1998) Yield and quality evaluations on a pair of processing tomato lines nearly isogenic for the Tm2a gene for resistance to the tobacco mosaic virus. *Euphytica*, **99**, 77–83. Available at: https://link.springer.com/article/10.1023/A:1018320232663 [Accessed July 4, 2021].

Underwood, C.J., Choi, K., Lambing, C., et al. (2018) Epigenetic activation of meiotic recombination near Arabidopsis thaliana centromeres via loss of H3K9me2 and non-CG DNA methylation. *Genome Res.*, **28**, 519–531. Available at: http://genome.cshlp.org/lookup/doi/10.1101/gr.227116.117 [Accessed March 30, 2018].

Vaillancourt, B. and Buell, C.R. (2019) High molecular weight DNA isolation method from diverse plant species for use with Oxford Nanopore sequencing. *bioRxiv*, 783159. Available at: https://doi.org/10.1101/783159 [Accessed July 4, 2021].

Vanburen, R., Bryant, D., Edger, P.P., et al. (2015) Single-molecule sequencing of the desiccation-tolerant grass Oropetium thomaeum. *Nature*, **527**, 508–511. Available at: https://github.com/PacificBiosciences/ [Accessed July 4, 2021].

Vaser, R., Sović, I., Nagarajan, N. and Šikić, M. (2017) Fast and accurate de novo genome assembly from long uncorrected reads. *Genome Res.*, **27**, 737–746. Available at: https://pubmed.ncbi.nlm.nih.gov/28100585/ [Accessed November 11, 2020].

Vilanova, S., Alonso, D., Gramazio, P., et al. (2020) SILEX: A fast and inexpensive high-quality DNA extraction method suitable for multiple sequencing platforms and recalcitrant plant species. *Plant Methods*, **16**, 1–11. Available at: https://doi.org/10.1186/s13007-020-00652-y [Accessed July 4, 2021].

Vollger, M.R., Logsdon, G.A., Audano, P.A., et al. (2020) Improved assembly and variant detection of a haploid human genome using single-molecule, high-fidelity long reads. *Ann. Hum. Genet.*, **84**, 125–140. Available at: https://pubmed.ncbi.nlm.nih.gov/31711268/ [Accessed July 4, 2021].

Wang, J., Chen, T., Han, M., et al. (2020) Plant NLR immune receptor Tm-22 activation requires NB-ARC domain-mediated self-association of CC domain. *PLoS Pathog.*, **16**, e1008475. Available at: https://doi.org/10.1371/journal.ppat.1008475 [Accessed July 4, 2021].

Wang, X., Gao, L., Jiao, C., et al. (2020) Genome of Solanum pimpinellifolium provides insights into structural variants during tomato breeding. *Nat. Commun.*, **11**. Available at: https://pubmed.ncbi.nlm.nih.gov/33199703/ [Accessed July 4, 2021].

Wang, Y., Rengs, W.M.J. Van, Zaidan, M.W.A.M. and Underwood, C.J. (2021) Meiosis in crops: From genes to genomes. *J. Exp. Bot.*, **72**, 6091–6109. Available at: https://academic.oup.com/jxb/advance-article/doi/10.1093/jxb/erab217/6278305 [Accessed August 30, 2021].

Zapata, L., Ding, J., Willing, E.M., et al. (2016) Chromosome-level assembly of Arabidopsis thaliana Ler reveals the extent of translocation and inversion polymorphisms. *Proc. Natl. Acad. Sci. U. S. A.*, **113**, E4052–E4060. Available at: http://www.ncbi.nlm.nih.gov/pubmed/27354520 [Accessed November 26, 2017].

Zhao, M., Ku, J.C., Liu, B., et al. (2021) The mop1 mutation affects the recombination landscape in maize. *Proc. Natl. Acad. Sci. U. S. A.*, **118**, 2009475118. Available at: https://www.pnas.org/content/118/7/e2009475118 [Accessed August 19, 2021].

Zhong, X.B., Fransz, P.F., Eden, J.W. Van, Ramanna, M.S., Kammen, A. Van, Zabel, P. and Hans de Jong, J. (1998) FISH studies reveal the molecular and chromosomal organization of individual telomere domains in tomato. *Plant J.*, **13**, 507–517.

Zhu, G., Wang, S., Huang, Z., et al. (2018) Rewiring of the Fruit Metabolome in Tomato Breeding. *Cell*, **172**, 249-261.e12. Available at: https://pubmed.ncbi.nlm.nih.gov/29328914/ [Accessed July 4, 2021].

Figure legends

Figure 1. A "long-read-only" assembly of the tomato genome

a, Workflow schematic of the MbTMV assembly process by merging individual and complementary assemblies from PacBio HiFi and ONT sequencing data. Created with BioRender.com b, D-GENIES alignment of the MbTMV assembly against the SL4.0 assembly. Chromosome names were shortened to "ch01-ch12" for convenience, min identity (abs) was set to 0.65. All chromosomes show near perfect alignment except for ch09. The x-axis represents the position on the MbTMV genome, where M is megabase pairs. c, the 12 chromosomes of Moneyberg-TMV paired at diakinesis of the first meiotic division.

Figure 2. Validation of MbTMV assembly

a, Omni-C interaction plot (Hi-C plot as plotted by Juicebox) demonstrating strong interactions within each chromosome of MbTMV. b, Circos plot of the MbTMV assembly including coverage of raw reads and location of genomic elements. From inner to outer ring: Ring 1 - ONT read coverage (cyan); Ring 2 - 45S rDNA intergenic spacer (IGS) (light blue); Ring 3 - telomeric repeat (pink), 5S rDNA sequence (dark blue), 45S rDNA (light green); Ring 4 – PacBio HiFi read coverage (red); Ring 5 – TGR3 (yellow); Ring 6 – TGR2 (light blue); Ring 7 – TGR1 (pink), TGR4 centromeric repeat (yellow) c, Chromosome lengths plot of MbTMV assembly and previously published assemblies: *S. lycopersicum* cv. 'Heinz 1706' (SL4.0), *S. pennellii* 'LA0716' and *S. pimpinellifolium* 'LA2093'. d, Synteny and Rearrangement (SyRI) plot of all 12 MbTMV chromosomes (Query) against all 12 SL4.0 chromosomes (Ref). All chromosomes show high synteny except for chromosome 9. Non-syntenic (non-matching) regions are shown as white gaps between Ref and Query. e, Self alignment and dot plot analysis of the full length of MbTMV chromosome 5. f, Self alignment and dot plot analysis of a 4 Mb region of MbTMV chromosome 5 containing the centromere, including identified TGR4 copies (orange), in 1 Mb windows.

Figure 3. Linkage drag of *S. peruvianum* derived sequence on chromosome 9

a, Synteny and Rearrangement (SyRI) plot of MbTMV chromosome 9 (Query) aligned against SL4.0 chromosome 9 (Ref). b, SyRI plot of ~10 Mbp region including TMV resistance gene locus. c, SyRI plot of ~1 Mbp region including TMV resistance gene locus. For a, b and c, re-alignments were performed on the specific regions and genomic positions (in Mb) are indicated on SL4.0 (Ref) and MbTMV (Query). M-1, M-TM2^2 and M-2 indicate genetic markers used in Figure 4b. Non-syntenic (non-matching) regions are shown as white gaps between Ref and Query. d, MbTMV, MmTMV (Moneymaker-TMV) and Merlice variant calling against SL4.0. SNP frequency (calculated in a 10kb window) plotted over the first 10 Mbp and last 13.5 Mbp of SL4.0 chromosome 9. *S. peruvianum* introgression was identified by increased SNP frequency. The two dotted vertical lines indicate introgression start and endpoints for MbTMV and MmTMV.

Figure 4. Genotyping and haplotyping-by-sequencing of the TM2^2 gene introgression in commercial tomato hybrids

a, Fruit phenotypes of tomato varieties used in this study. Top row, from left: Growdena, Maxeza, Tomagino; Bottom row, from left: Sevance, Funtelle, Moneyberg-TMV x Microtom F1 hybrid, Moneyberg-TMV, Microtom. b, Marker studies on the TMV resistance introgression from *S. peruvianum* including 5 commercial hybrids: Maxeza (Truss tomato), Tomagino (Cherry tomato), Funtelle (Date tomato), Growdena (Beefsteak tomato) and Sevance (“on the vine” tomato), 2 inbred lines resistant to TMV (LYC1969 and Moneyberg-TMV) and 2 inbred lines susceptible to TMV (Heinz 1706 and Microtom). Marker locations of markers M-1, M-TM2^2 and M-2 are shown in Figure 3a. c, workflow schematic of Funtelle Flye assembly for both chromosome 9 haplotypes. Created with BioRender.com. d, D-GENIES plot of the Funtelle Flye assembly contigs (right), competitvely aligned against both SL4.0 chromosome 9 (top left) and MbTMV chromosome 9 (top right). Min identity (abs) was set to 0.65 and small matches were completely filtered out.

Table 1) Statistics of different sequencing methods

Table 1 shows the total sequencing output and summary statistics for two cells of PacBio HiFi data and two cells of ONT PromethION data, before quality filtering.

	PacBio			Oxford Nanopore Technologies		
	Run_1	Run_2	Combined	Run_1	Run_2	Combined
Number of sequences	1,356,407	867,228	2,223,635	4,597,421	4,522,199	9,119,620
Output (Gbp)	18.8	21.8	40.6	100.5	101.1	201.6
Longest read (kbp)	31.3	50.3	50.3	862.3	629.5	862.3
Median read length (kbp)	13.9	24.3	14.7	13.1	13.6	13.4
Mean read length (kbp)	13.9	25.1	18.3	21.9	22.4	22.1
N50 read length (kbp)	13.9	24.8	21.1	41.6	42.4	42.0
Mean quality score	28.59	24.65	26.06	11.28	11.18	11.23

Table 2) Statistics of different assembly methods

Table 2 shows the summary statistics for assemblies obtained from PacBio and ONT data, respectively. The Flye + NECAT merged assembly presented here does not include polishing of the merged assembly with PacBio data (see Materials and methods). BUSCO analysis of the completeness of gene content is using the *Solanales* benchmark set.

Input data	40.6 Gbp (PacBio HiFi)			165.7 Gbp (ONT)		
Assembly	Hifiasm	Canu	Hifiasm + Canu	Flye	NECAT	Flye + NECAT
Number of contigs	750	2396	731	371	125	105
Cumulative size (Mbp)	868.9	928.7	871.9	809.7	829.6	829.1
N50 (Mbp)	31.3	17.0	36.8	18.9	50.2	53.4
N90 (Mbp)	8.7	0.08	9.1	5.4	10.6	18.6
L50	10	14	9	15	7	7
L90	32	170	31	45	21	15
Longest contig (Mbp)	66.6	66.7	66.8	47.0	74.2	82.8
BUSCO (genes searched)	5950	5950	5950	5950	5950	5950
BUSCO (complete)	5852	5853	5852	5820	5779	5824
BUSCO (complete) %	98.4	98.4	98.4	97.8	97.1	97.9
BUSCO (complete single)	5739	5735	5739	5703	5666	5713
BUSCO (complete duplicated)	113	118	113	117	113	111
BUSCO (fragmented)	12	12	12	21	38	17
BUSCO (missing)	86	85	86	109	133	109
LAI	13.48	9.65	13.43	10.63	10.39	10.58
raw LAI	7.85	4.02	7.80	5.00	4.76	4.95

Table 3) Statistics of different assemblies

Table 3 shows the summary statistics for the MbTMV assembly and three "gold standard" tomato species genome assemblies: 'Heinz 1706' SL4.0 (Hosmani *et al.*, 2019), *S. pimpinellifolium* 'LA2093' (X., Wang *et al.*, 2020) *and S. pennellii* 'LA0716' (Bolger *et al.*, 2014). BUSCO analysis of the completeness of gene content is using the *Solanales* benchmark set.

Assembly name	MbTMV	SL4.0	LA2093	LA0716
PacBio assembly	HiFiasm v0.14.2; Canu v2.1.1	Canu v1.5	Canu v1.7.1	-
ONT assembly	NECAT ; Flye	-	-	-
Polishing	Medaka (ONT); Racon (HiFi)	PacBio + Illumina	PacBio + Illumina	Illumina
Scaffolding	-	HiC	HiC	Genetic map
Number of sequences	13	13	13	13
Sequences >50 Mbp	12	11	11	13
Cumulative size (Mbp)	833.0	782.5	810.5	989.5
N50 (Mbp)	68.5	65.3	67.2	78
N90 (Mbp)	54.7	53.5	55.6	60.7
L50	6	6	6	6
L90	11	11	11	12
Maximum contig size (Mbp)	96.5	90.9	95.5	109.3
Ns per 100 kbp	0.64	5.72	357.21	11533.09
BUSCO (genes searched)	5950	5950	5950	5950
BUSCO (complete)	5853	5825	5854	5847
BUSCO (complete) %	98.4	97.8	98.4	98.3
BUSCO (complete single)	5743	5718	5744	5711
BUSCO (complete duplicated)	110	107	110	136
BUSCO (fragmented)	12	24	11	17
BUSCO (missing)	85	101	85	86
LAI	13.43	10.39	13.18	7.70
raw LAI	7.80	4.76	7.55	2.07

Fig.1: A “long-read-only” assembly of the tomato genome

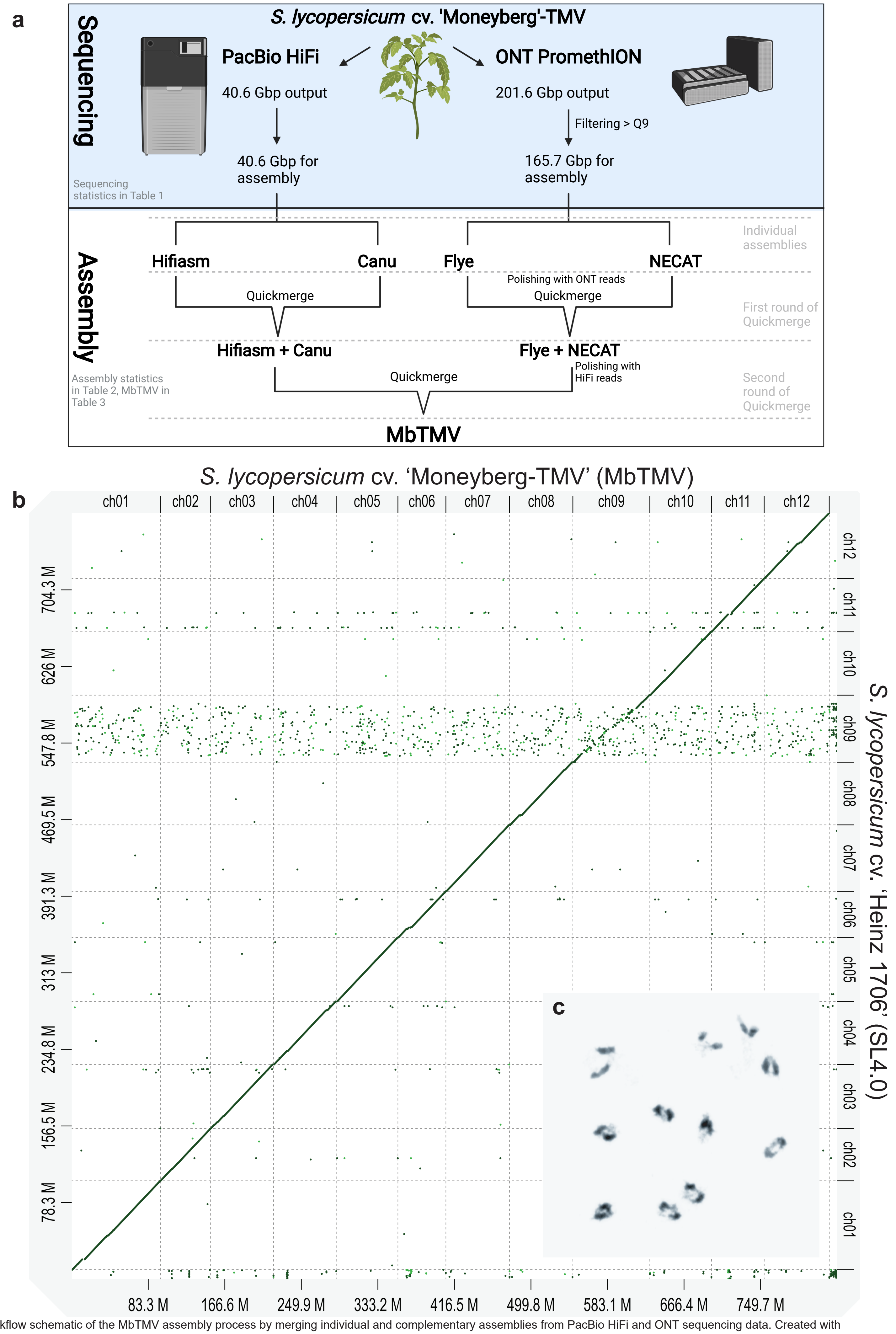

a, Workflow schematic of the MbTMV assembly process by merging individual and complementary assemblies from PacBio HiFi and ONT sequencing data. Created with BioRender.com **b**, D-GENIES alignment of the MbTMV assembly against the SL4.0 assembly. Chromosome names were shortened to “ch01-ch12” for convenience, min identity (abs) was set to 0.65. All chromosomes show near perfect alignment except for ch09. The x-axis represents the position on the MbTMV genome, where M is megabase pairs. **c**, the 12 chromosomes of Moneyberg-TMV paired at diakinesis of the first meiotic division.

Fig.2: Validation of MbTMV assembly

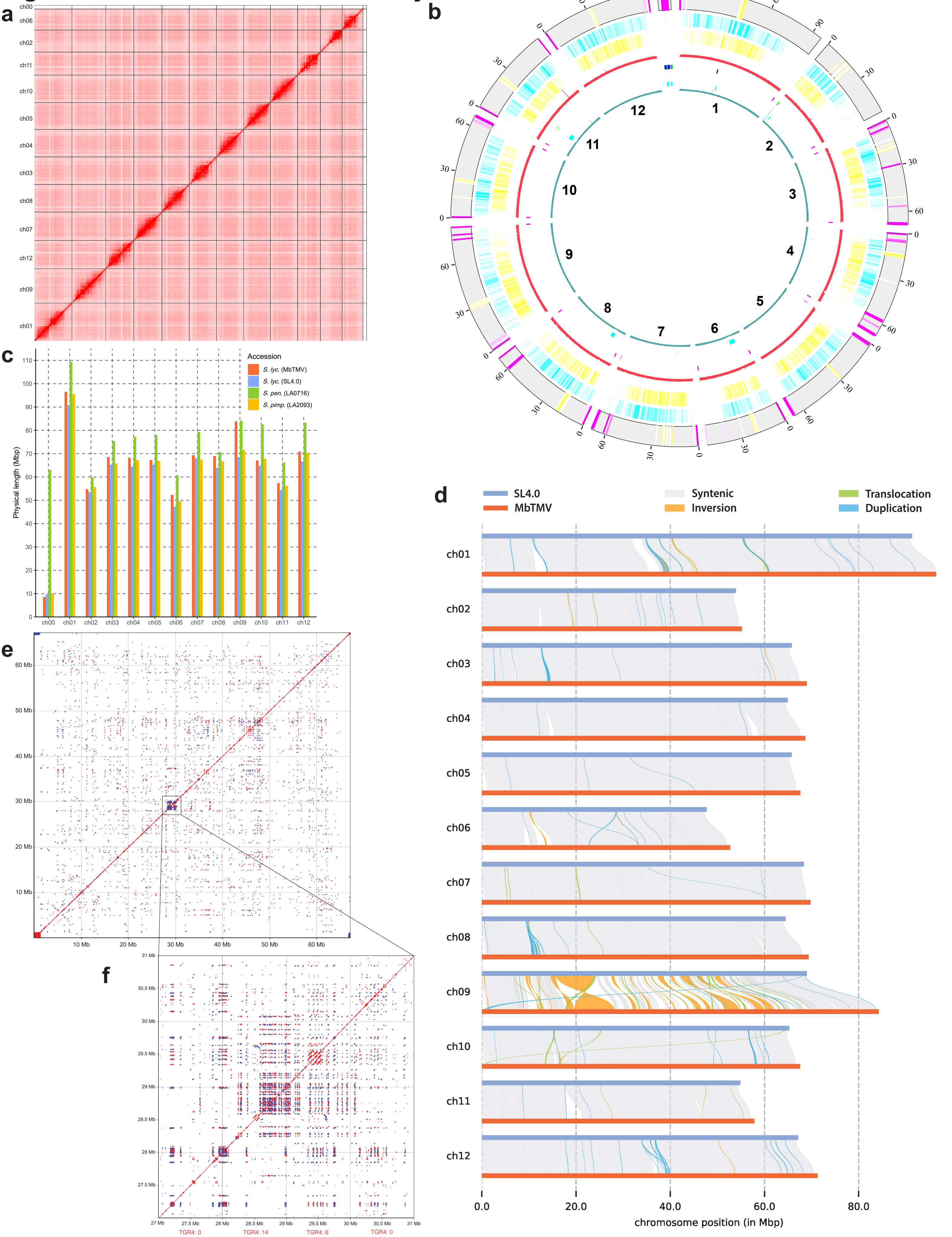

a, Omni-C interaction plot (Hi-C plot as plotted by Juicebox) demonstrating strong interactions within each chromosome of MbTMV. **b**, Circos plot of the MbTMV assembly including coverage of raw reads and location of genomic elements. From inner to outer ring: Ring 1 - ONT read coverage (cyan); Ring 2 - 45S rDNA intergenic spacer (IGS) (light blue); Ring 3 - telomeric repeat (pink), 5S rDNA sequence (dark blue), 45S rDNA (light green); Ring 4 – PacBio HiFi read coverage (red); Ring 5 – TGR3 (yellow); Ring 6 – TGR2 (light blue); Ring 7 – TGR1 (pink), TGR4 centromeric repeat (yellow) **c**, Chromosome lengths plot of MbTMV assembly and previously published assemblies: *S. lycopersicum* cv. 'Heinz 1706' (SL4.0), *S. pennellii* 'LA0716' and *S. pimpinellifolium* 'LA2093'. **d**, Synteny and Rearrangement (SyRI) plot of all 12 MbTMV chromosomes (Query) against all 12 SL4.0 chromosomes (Ref). All chromosomes show high synteny except for chromosome 9. Non-syntenic (non-matching) regions are shown as white gaps between Ref and Query. **e**, Self alignment and dot plot analysis of the full length of MbTMV chromosome 5. **f**, Self alignment and dot plot analysis of a 4 Mb region of MbTMV chromosome 5 containing the centromere, including identified TGR4 copies (orange), in 1 Mb windows.

Fig.3: Linkage drag of *S. peruvianum* derived sequence on chromosome 9

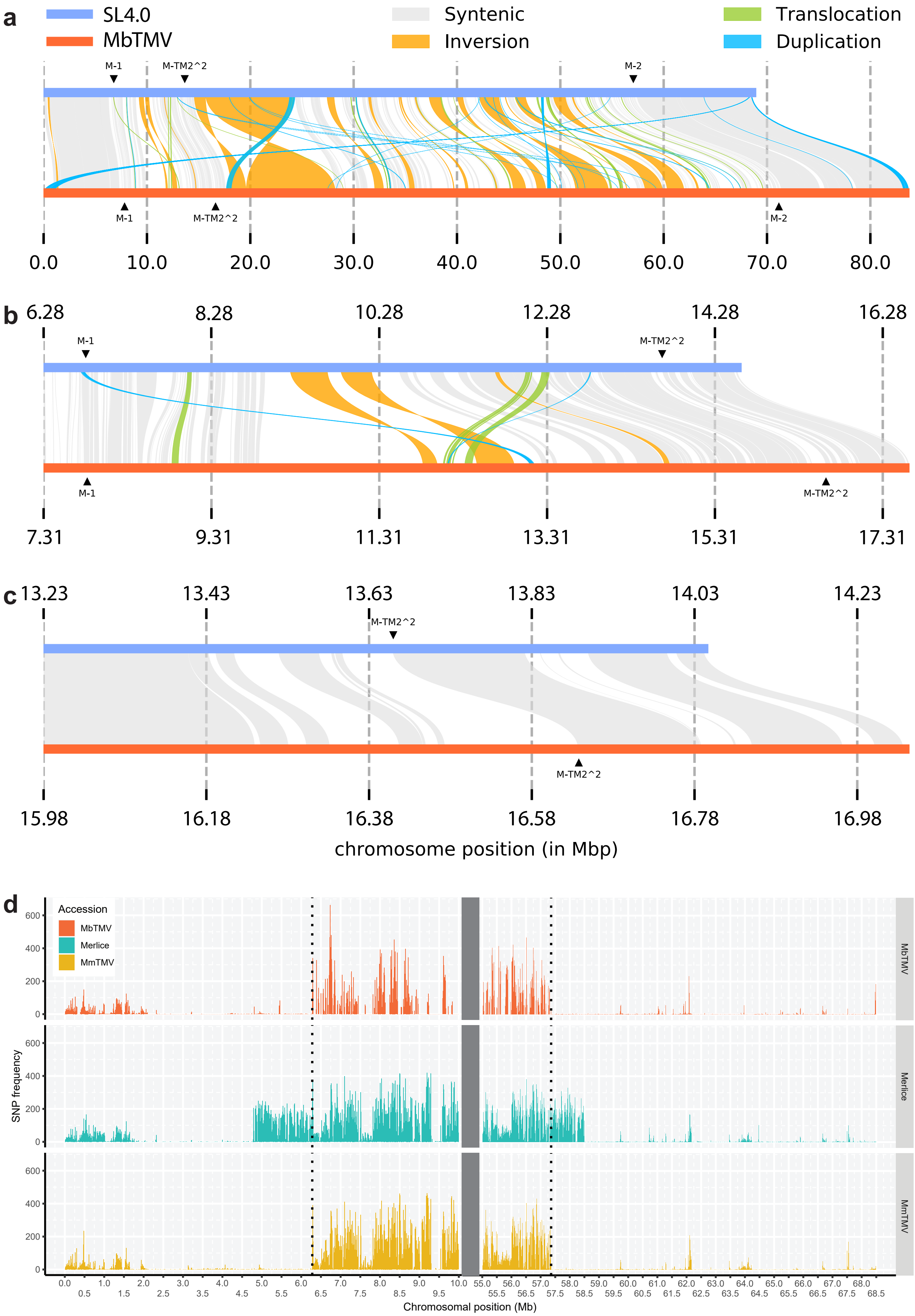

a, Synteny and Rearrangement (SyRI) plot of MbTMV chromosome 9 (Query) aligned against SL4.0 chromosome 9 (Ref). **b**, SyRI plot of ~10 Mbp region including TMV resistance gene locus. **c**, SyRI plot of ~1 Mbp region including TMV resistance gene locus. For **a**, **b** and **c**, re-alignments were performed on the specific regions and genomic positions (in Mb) are indicated on SL4.0 (Ref) and MbTMV (Query). M-1, M-TM2^2 and M-2 indicate genetic markers used in Figure 4b. Non-syntenic (non-matching) regions are shown as white gaps between Ref and Query. **d**, MbTMV, MmTMV (Moneymaker-TMV) and Merlice variant calling against SL4.0. SNP frequency (calculated in a 10kb window) plotted over the first 10 Mbp and last 13.5 Mbp of SL4.0 chromosome 9. *S. peruvianum* introgression was identified by increased SNP frequency. The two dotted vertical lines indicate introgression start and endpoints for MbTMV and MmTMV.

Fig.4: Genotyping and haplotyping-by-sequencing of the *TM2^2* gene introgression in commercial tomato hybrids

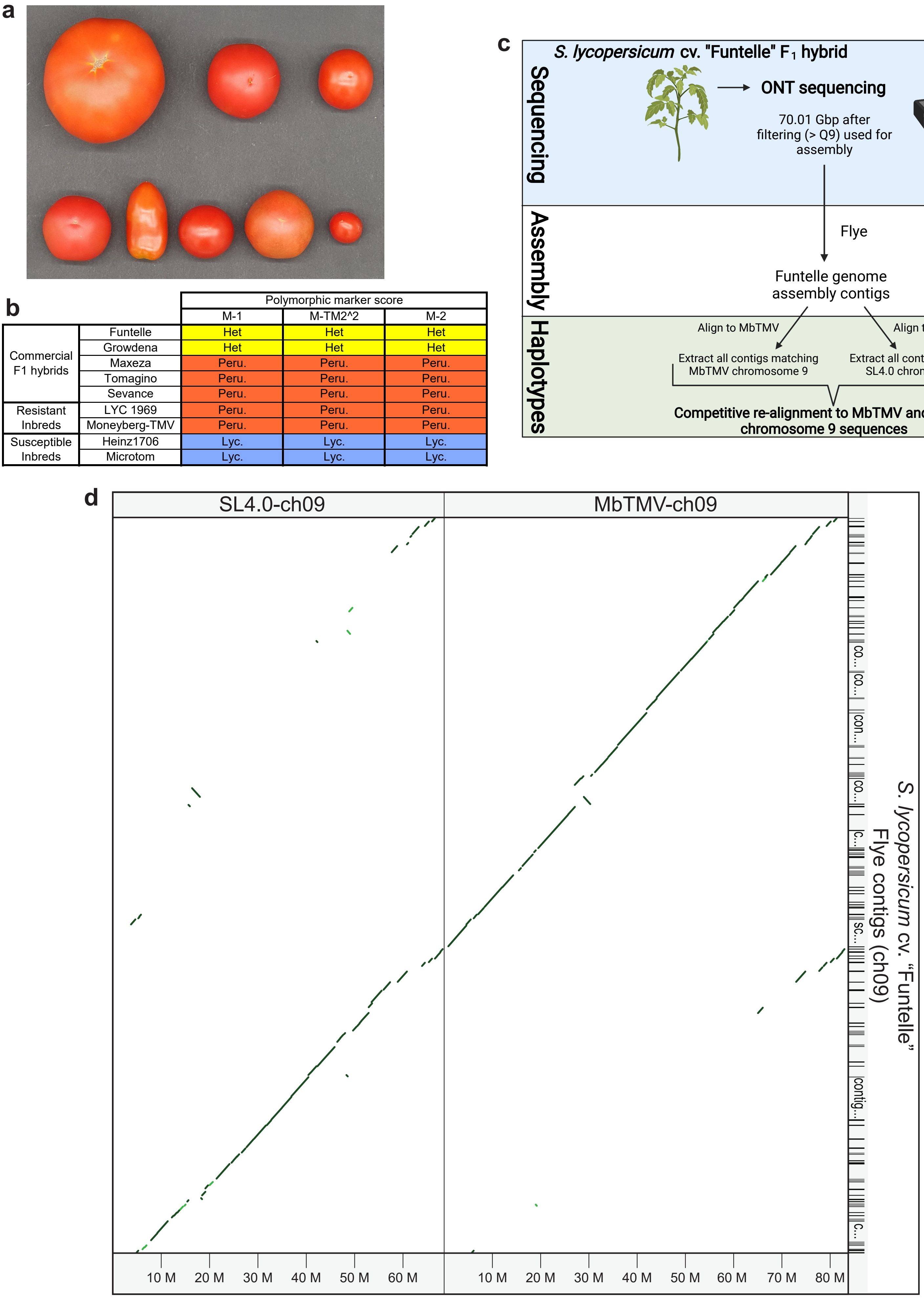

		Polymorphic marker score		
		M-1	M-TM2^2	M-2
Commercial F1 hybrids	Funtelle	Het	Het	Het
	Growdena	Het	Het	Het
	Maxeza	Peru.	Peru.	Peru.
	Tomagino	Peru.	Peru.	Peru.
	Sevance	Peru.	Peru.	Peru.
Resistant Inbreds	LYC 1969	Peru.	Peru.	Peru.
	Moneyberg-TMV	Peru.	Peru.	Peru.
Susceptible Inbreds	Heinz1706	Lyc.	Lyc.	Lyc.
	Microtom	Lyc.	Lyc.	Lyc.

Sequencing

S. lycopersicum cv. "Funtelle" F₁ hybrid

ONT sequencing

70.01 Gbp after filtering (> Q9) used for assembly

Assembly

Flye

Funtelle genome assembly contigs

Haplotypes

Align to MbTMV

Align to SL4.0

Extract all contigs matching MbTMV chromosome 9

Extract all contigs matching SL4.0 chromosome 9

Competitive re-alignment to MbTMV and SL4.0 chromosome 9 sequences

a, Fruit phenotypes of tomato varieties used in this study. Top row, from left: Growdena, Maxeza, Tomagino; Bottom row, from left: Sevance, Funtelle, Moneyberg-TMV x Microtom F1 hybrid, Moneyberg-TMV, Microtom. **b**, Marker studies on the TMV resistance introgression from *S. peruvianum* including 5 commercial hybrids: Maxeza (Truss tomato), Tomagino (Cherry tomato), Funtelle (Date tomato), Growdena (Beefsteak tomato) and Sevance ("on the vine" tomato), 2 inbred lines resistant to TMV (LYC1969 and Moneyberg-TMV) and 2 inbred lines susceptible to TMV (Heinz 1706 and Microtom). Marker locations of markers M-1, M-TM2^2 and M-2 are shown in Figure 3a. **c**, workflow schematic of Funtelle Flye assembly for both chromosome 9 haplotypes. Created with BioRender.com. **d**, D-GENIES plot of the Funtelle Flye assembly contigs (right), competitvely aligned against both SL4.0 chromosome 9 (top left) and MbTMV chromosome 9 (top right). Min identity (abs) was set to 0.65 and small matches were completely filtered out.